SUPPLEMENTARY INFORMATION FOR

Robust *de novo* designed homotetrameric coiled coils

Caitlin L. Edgell [a,b], Nigel J. Savery [b,c] and Derek N. Woolfson *[,a,b,c]

[a] School of Chemistry, University of Bristol, Bristol, BS8 1TS, United Kingdom
[b] School of Biochemistry, University of Bristol, Bristol, BS8 1TD, United Kingdom
[c] BrisSynBio, Life Sciences Building, University of Bristol, Bristol, BS8 1TQ, United Kingdom

* Corresponding author: Derek N. Woolfson
Email: D.N.Woolfson@bristol.ac.uk

This file includes:

MATERIALS AND METHODS:

General

All biophysical characterisation was performed in phosphate buffered saline (8.2 mM Na_2HPO_4, 1.8 mM KH_2PO_4, 137 mM NaCl, 2.7 mM KCl, pH 7.4) unless otherwise stated. Chemicals and solvents were obtained from Fisher Scientific or Sigma Aldrich unless otherwise stated.

Coiled coil design

The sequences of the peptides CC-Tet-KE and CC-Tet-3 were based on the homotetrameric coiled coil CC-Tet. CC-Tet-KE was designed by swapping the identities of the charged residues at the *e* and *g* positions in CC-Tet. The sequence is otherwise identical, including a *C*-terminal AG mass tag used for peptide identification. CC-Tet-3 was designed by removing the first heptad, after the *N*-terminal Gly, and the *C*-terminal AG mass tag from CC-Tet.

The peptides 1-EK-4, 1-KE-4, 2-EK-4, 2-KE-4, 3-EK-4, 3-KE-4, 4-EK-4, 4-KE-4, 1-EK-3, 2-EK-3, 3-EK-3, 4-EK-3, 4-EK-3.5-N, 4-EK-3.5-C, 4-KE-3, 4-KE-3.5-N and 4-KE-3.5-C were designed to contain different configurations of Glu and Lys pairs at various core-flanking heptad positions. Peptides 1-EK-4, 1-KE-4 and 1-EK-3 contained *e*/*g* pairs where in 1-EK-4 and 1-EK-3 *g*=Glu, *e*=Lys and in 1-KE-4 *g*=Lys, *e*=Glu. Peptides 2-EK-4, 2-KE-4 and 2-EK-3 contained *c*/*e* pairs where in 2-EK-4 and 2-EK-3 *c*=Glu, *e*=Lys and in 2-KE-4 *c*=Lys, *e*=Glu. Peptides 3-EK-4, 3-KE-4 and 3-EK-3 contained *g*/*b* ionic pairs where in 3-EK-4 and 3-EK-3 *g*=Glu, *b*=Lys and in 3-KE-4 *g*=Lys, *b*=Glu. Peptides 4-EK-4, 4-KE-4, 4-EK-3, 4-EK-3.5-N, 4-EK-3.5-C, 4-KE-3, 4-KE-3.5-N and 4-KE-3.5-C contained *b*/*c* ionic pairs where in 4-EK-4 , 4-EK-3, 4-EK-3.5-N and 4-EK-3.5-C *b*=Glu, *c*=Lys and in 4-KE-4, 4-KE-3, 4-KE-3.5-N and 4-KE-3.5-C *b*=Lys, *c*=Glu. Where *e* or *g* positions were not Glu or Lys, these positions were made Gln. Where *b* or *c* positions were not Glu or Lys, these positions were made Ala. All peptides were designed in *c*-register (*i.e.* excepting capping Gly residues at the *C* and *N* termini, the peptide sequences begin at *c* positions, respectively), except 4-EK-3.5-N, which was designed in *g*-register. All peptides contained *a*=Leu/*d*=Ile cores and were designed to be 3-, 3.5- or 4-heptads long. The *f* positions were populated by Gln (or Lys, where required to promote solubility) and a single Trp to provide a chromophore. Helix-capping Gly residues were added to *N* and *C* termini.

Solid-phase peptide synthesis

Peptides were synthesised on a 0.1 mmol scale by solid-phase peptide synthesis on ChemMatrix Rink amide resin (PCAS BioMatrix) or Novabiochem Rink amide resin (Merck) on a Liberty Blue automated microwave peptide synthesiser (CEM) using Fmoc-protected amino acids (supplied by Novabiochem or Cambridge Reagents) at 0.2 M in dimethylformamide (DMF, Cambridge Reagents). Deprotection was performed with 20 % (v/v) morpholine (Alfa Aesar) in DMF. Coupling was performed using 0.5 M 6-Chloro-1-hydroxybenzotriazole (Cambridge Reagents) in DMF as the activator and 1.0 M N,N′-Diisopropylcarbodiimide (DIC, Acros Organics) in DMF as the activator base. Following synthesis, peptides were N-terminally acetylated for 20 min at room temperature using 1 % (v/v) acetic anhydride and 1 % (v/v) pyridine in 1:1 DMF/dichloromethane (DCM, Sigma Aldrich) or 100 % DMF. Peptides were simultaneously cleaved from the resin and side chain deprotected for 2 h at room temperature using a mixture of 5 % (v/v) H2O and 5 % (v/v) triisopropylsaline (TIPS, Acros Organics) in trifluoroacetic acid (TFA, Acros Organics). Resin was removed by filtration and crude peptides were precipitated in cold diethyl ether (Honeywell Research Chemicals) then isolated by centrifugation. Peptides were re-suspended in 1:1 ultrapure Milli-Q water/acetonitrile then lyophilised prior to purification.

Peptide purification

Peptides were purified by reversed-phase high-performance liquid chromatography (HPLC) using C18 reversed phase columns (150 x 10 mm, 100 Å pore size, Phenomenex). Linear gradients of buffer A (ultrapure Milli-Q water containing 0.1 % (v/v) TFA) and buffer B (acetonitrile containing 0.1 % (v/v) TFA) were used. Typically, a linear gradient of 20–80 % buffer B over 30 min at room temperature was used. Columns were equilibrated at the starting buffer conditions and washed with 95 % buffer B between gradients. Product fractions were collected manually. Peptide masses were confirmed by MALDI-TOF mass spectrometry with an ultrafleXtreme II mass spectrometer in positive-ion reflector mode (Bruker, UK). Samples were air-dried onto a ground-steel target plate with α-cyano-4-hydroxycinnamic acid matrix (α-CHCA, Fluka Analytical). Representative mass spectra are shown in Figure S2. Fraction purity was confirmed by reversed-phase HPLC using analytical C18 reversed-phase columns (100 x 4.6 mm, 100 Å pore size, Phenomenex) with linear gradients of buffer A and B. Representative analytical HPLC traces are shown in Figure S3. Selected fractions were pooled and lyophilised prior to biophysical characterisation.

Circular dichroism spectroscopy

Circular dichroism (CD) spectroscopy was performed using either a JASCO J-810 or a JASCO J-815 spectropolarimeter with a Peltier temperature controller (Jasco, UK) using quartz cuvettes. Full spectra were measured between 190 and 260 nm with a 1 nm step size, 100 nm.min^{-1} scanning speed, 1 nm bandwidth and 1 second response time. Spectra were measured at 5 °C unless otherwise stated. Variable temperature experiments were performed by heating and cooling samples 5–95–5 °C at a rate of 40 °C.h^{-1} whilst monitoring CD at 222 nm at 0.5 °C intervals. Data was buffer subtracted then CD (mdeg) was converted to mean residue ellipticity (MRE, deg.cm^2.dmol^{-1}.res^{-1}) by normalising for peptide concentration, number of amide bonds and cuvette pathlength, according to Equation 1. Fraction helix (%) was calculated using Equation 2.[1]

$$\mathrm{MRE} = \frac{\mathrm{CD}}{10 \times c \times l \times n}$$

Equation 1 Equation for the conversion of CD (mdeg) to MRE (deg.cm^2.dmol^{-1}.res^{-1}). c, molar peptide concentration; l, sample path length in cm; n, number of amide bonds in sample (including C-terminal amide).

$$\text{Fraction helix (\%)} = 100 \times \frac{\mathrm{MRE}_{222} - \mathrm{MRE}_{\mathrm{coil}}}{-42500 \times \left(1 - {}^{3}/_{n}\right) - \mathrm{MRE}_{\mathrm{coil}}}$$

Equation 2 Equation for calculating fraction helix (%) from MRE at 222 nm (MRE_{222}, deg.cm^2.dmol^{-1}.res^{-1}). MREcoil = 640-45T; T, temperature (°C); n, number of amide bonds in sample (including C-terminal amide).

Representative CD spectra and variable temperature data are shown in Figures S4–S23.

Analytical ultracentrifugation

All analytical ultracentrifugation (AUC) experiments were performed at 20 °C in Beckman-Optima XL-I or XL-A analytical ultracentrifuges using An-50 or An-60 Ti rotors. For sedimentation velocity (SV) experiments, solutions were prepared in buffer at a total peptide concentration of 140 μM either at a volume of 305 μL and loaded into an SV cell with a 12 mm graphite-filled centrepiece and quartz windows, or at a volume of 410 μL and loaded into an SV cell with a 12 mm aluminium centrepiece and sapphire windows. The reference channels of the graphite and aluminium centrepieces were loaded with 320 μL or 420 μL of buffer, respectively. All measurements were performed in PBS (pH 7.4; density, ρ = 1.0054 g/cm2; viscosity, η = 0.01002 P). Following temperature equilibration at 3 krpm, samples were spun at 50 or 60 krpm. A total of 120 absorbance scans at 280 nm over a radial range of approximately 5.8 to 7.3 cm were measured at 5-minute intervals. Data were fitted to a continuous c(s)

distribution model using Sedfit, at 99 % confidence level.[2] The baseline, meniscus, frictional ratio (f/f_0), and systematic time-invariant and radial-invariant noise were fitted. The partial specific volume ($\bar{v}$) for each peptide/peptide combination was calculated using Sedfit.[2] The buffer densities were calculated using SEDNTERP. For all SV experiments, residuals are shown below the c(s) distribution as a rectangular greyscale bitmap where the shade of grey indicates the magnitude of the difference between the data and the fit. Each residuals bitmap displays the residuals for every scan, stacked from top to bottom, across the entire radial range included in the data processing, where the left and right edges of the bitmap represent the data boundaries at the meniscus and cell bottom, respectively.

Sedimentation equilibrium (SE) experiments were preformed using 12 mm six-channel epon-charcoal equilibrium cells with quartz windows. Solutions were prepared in buffer at a total peptide concentration of 70 μM. Samples were spun at 21–42 krpm. Absorbance scans at 280 nm were measured at 3 or 4 krpm intervals following an initial equilibration period of 8 h and a second equilibration period of 1 h. Data sets were initially fitted to a single, ideal species model using Ultrascan II (http://www.ultrascan.uthscsa. edu/). 99 % confidence limits were calculated using Monte Carlo analysis of the obtained fits.

Peptide crystallography

Peptides were crystallised at 20 °C using the sitting drop method. Peptide solutions were prepared at 3.0 mM in unbuffered deionised water. Screening was carried out using the commercial screens JCSG-plusTM, Morpheus®, Structure Screen 1 & 2 and PACT premier™ (Molecular Dimensions). Screens were prepared in 96-well MRC plates using an Oryx8000 Protein Crystallisation Robot (Douglas Instruments) with reservoir volumes of 50 μL. Droplets contained 0.3 μL peptide solution equilibrated with 0.3 μL of reservoir solution. Single crystals were cryoprotected by soaking in 25 % (v/v) glycerol in ultrapure Milli-Q water and reservoir solution, prior to loop-mounting and plunge-freezing in N_2(l). Data collection was carried out under cryogenic conditions at wavelengths of 0.93 to 0.98 Å on beamline i03, or i04 at Diamond Light Source (Didcot, UK).

Data indexing and integration were carried out in MOSFLM and scaling was carried out in AIMLESS.[3,4] Initial phases for the peptide 2-EK-4 were determined by molecular replacement with Phaser-MR [5] using full or partial poly-alanine parallel tetrameric coiled-coil models (as predicted by the Matthews coefficient)[6] generated in ISAMBARD or CC-Builder as the search models.[7,8] The phase for the peptides 3-EK-4 and 4-KE-4 were generated using ARCIMBOLDO.[9] AIMLESS, Phaser-MR and ARCIMBOLDO were all used as implemented in CCP4.[10] Final models were obtained through iterative rounds of model building in COOT and refinement in PHENIX Refine.[11,12] All protein structure images were generated in PyMol (http://www.pymol.org).

SUPPLEMENTARY FIGURES AND TABLES

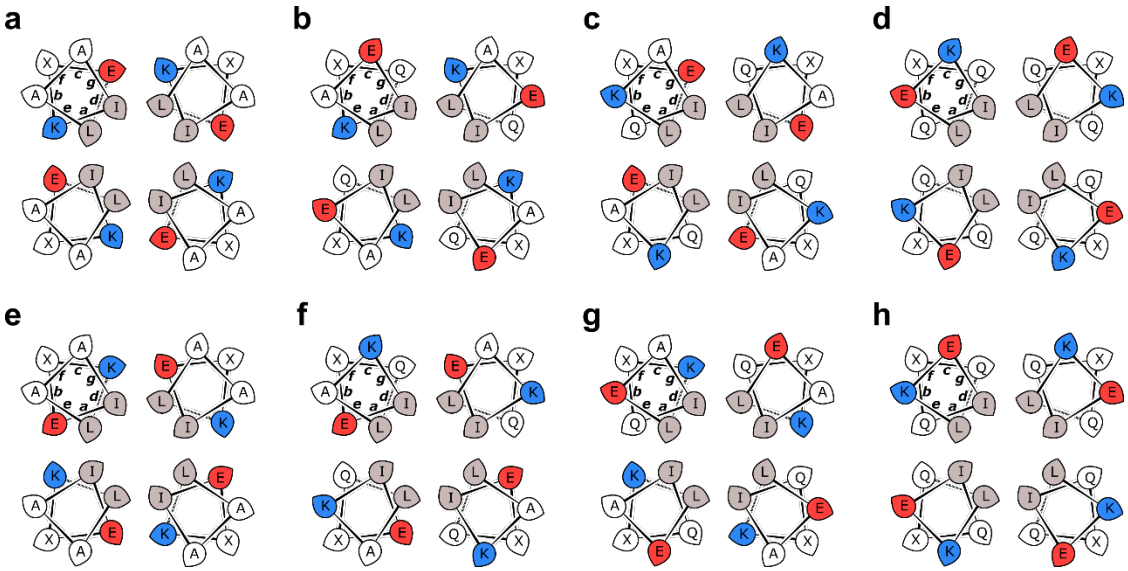

Figure S1 Helical wheels for (a) 1-EK-4, (b) 2-EK-4, (c) 3-EK-4, (d) 4-EK-4, (e) 1-KE-4, (f) 2-KE-4, (g) 3-KE-4 and (h) 4-KE-4, with heptad positions indicated.

1

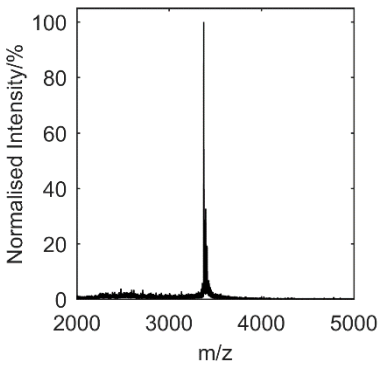

Exp.: 3374.993
Obs.: 3374.256

2

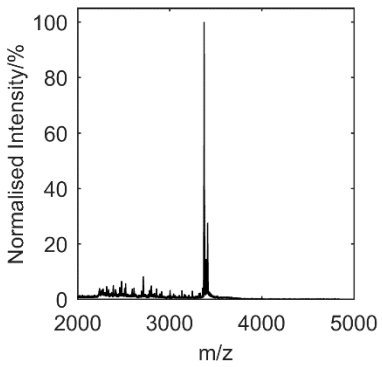

Exp.: 3374.993
Obs.: 3374.647

3

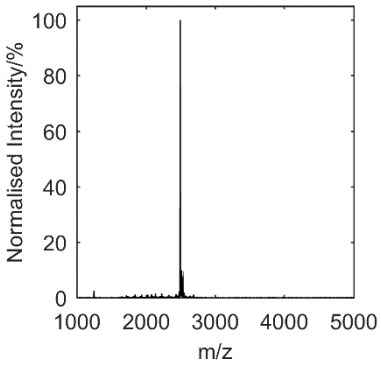

Exp.: 2492.967
Obs.: 2492.694

4

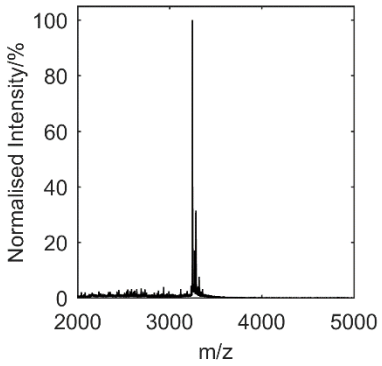

Exp.: 3246.95
Obs.: 3246.927

5

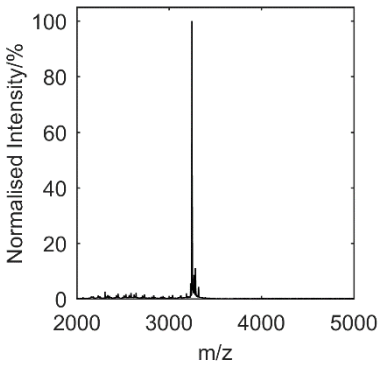

Exp.: 3246.82
Obs.: 3246.6

6

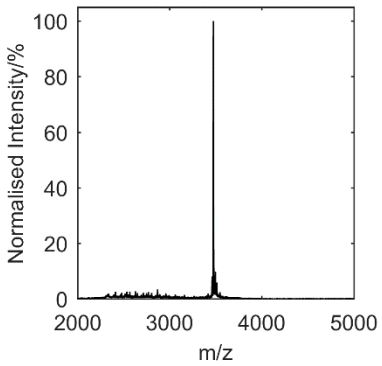

Exp.: 3475.027
Obs.: 3474.337

7

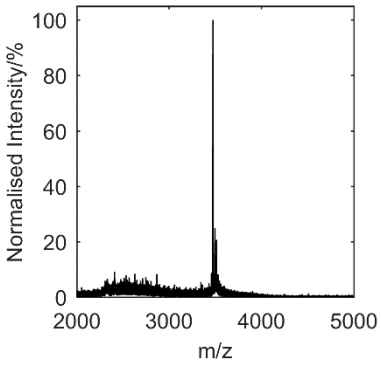

Exp.: 3475.027
Obs.: 3473.661

8

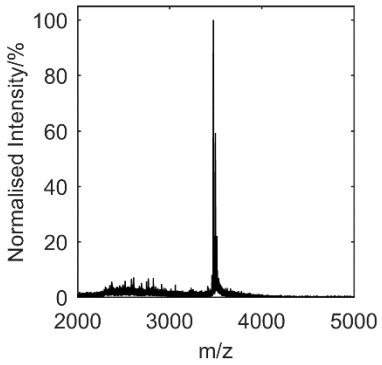

Exp.: 3475.027
Obs.: 3473.581

9

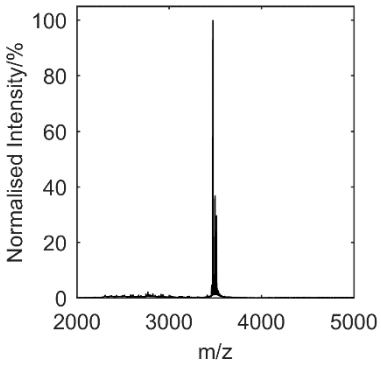

Exp.: 3475.027
Obs.: 3474.177

10

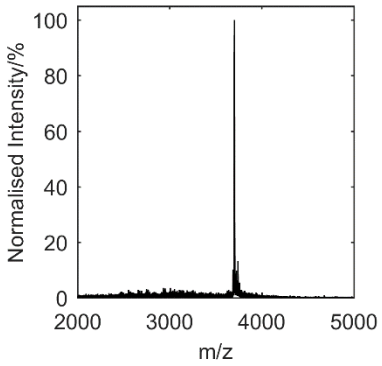

Exp.: 3703.364
Obs.: 3703.117

11

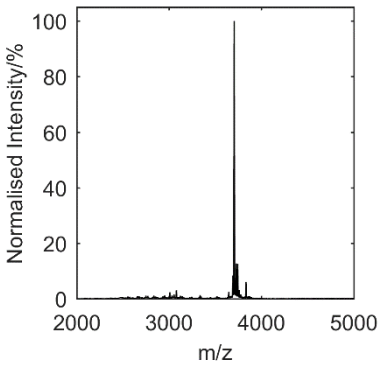

Exp.: 3703.364
Obs.: 3704.233

12

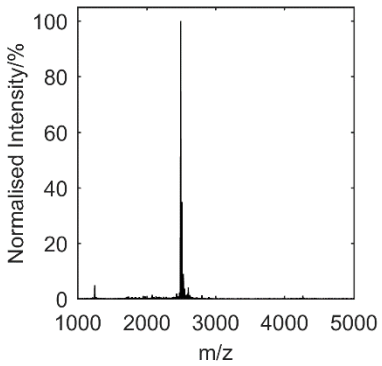

Exp.: 2493.011
Obs.: 2491.701

13

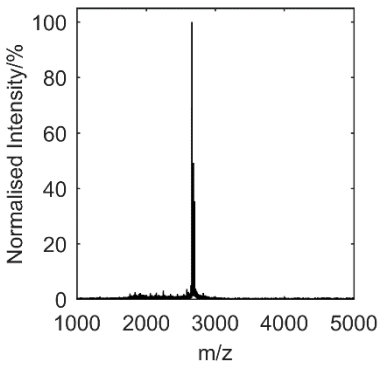

Exp.: 2664.08
Obs.: 2662.527

14

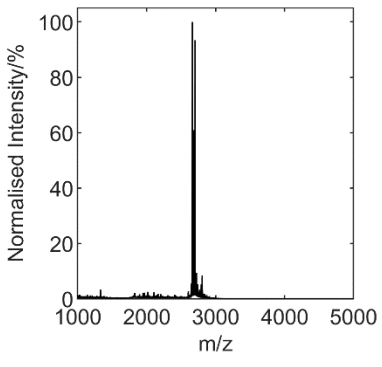

Exp.: 2664.08
Obs.: 2662.437

15

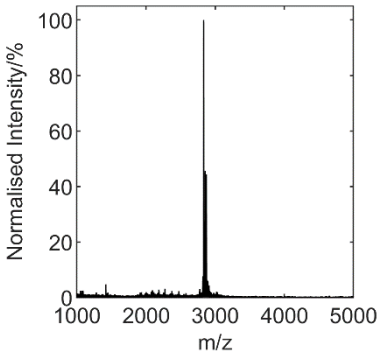

Exp.: 2835.322
Obs.: 2833.682

16

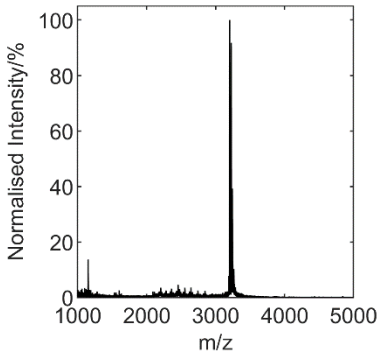

Exp.: 3205.727
Obs.: 3203.75

17

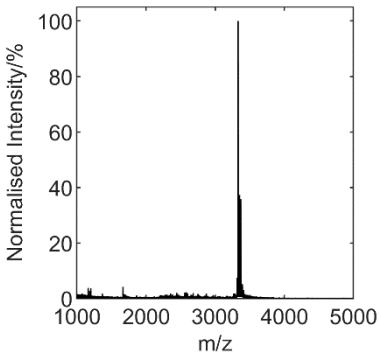

Exp.: 3332.959
Obs.: 3330.883

18

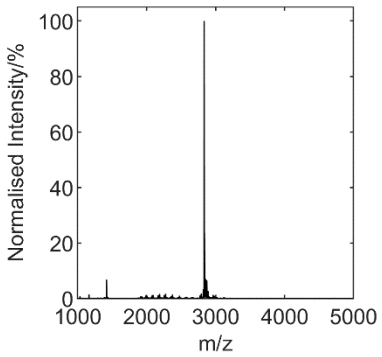

Exp.: 2835.322
Obs.: 3833.842

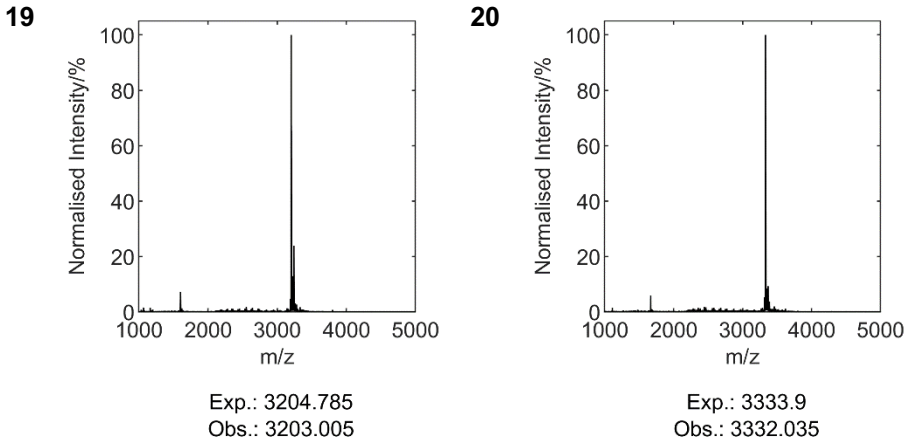

Figure S2 Representative mass spectra of all discussed peptides. Peptides numbered as in Table S1. Exp, expected mass (Da); obs, observed mass (Da); m/z, mass:charge ratio.

1

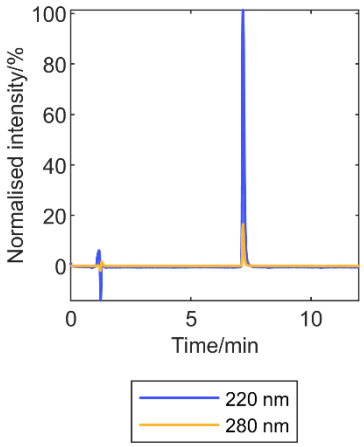
Normalised intensity/%
Time/min
220 nm
280 nm

2

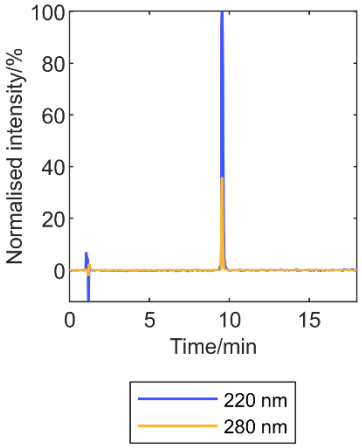
Normalised intensity/%
Time/min
220 nm
280 nm

3

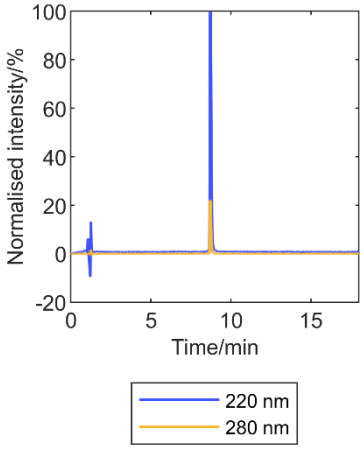
Normalised intensity/%
Time/min
220 nm
280 nm

4

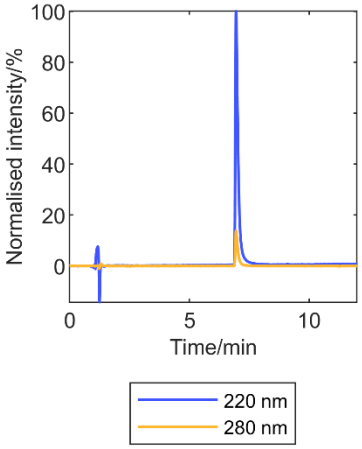
Normalised intensity/%
Time/min
220 nm
280 nm

5

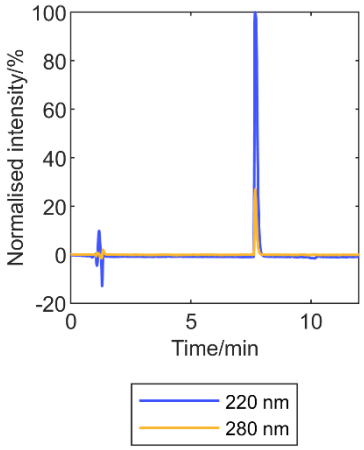
Normalised intensity/%
Time/min
220 nm
280 nm

6

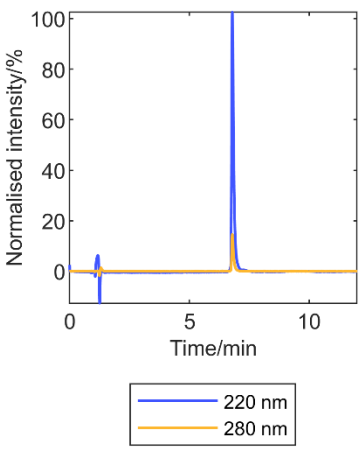
Normalised intensity/%
Time/min
220 nm
280 nm

7

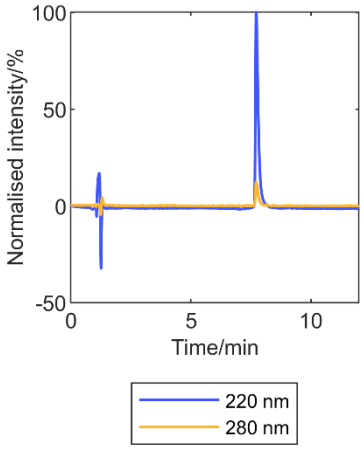
Normalised intensity/%
100
50
0
-50
0
5
10
Time/min
220 nm
280 nm

8

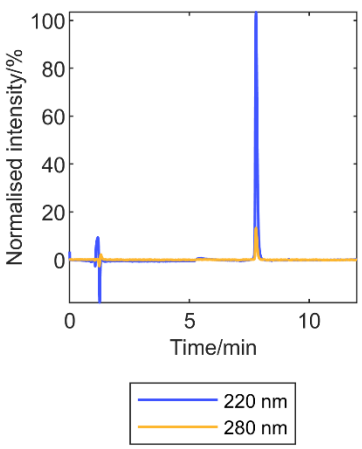
Normalised intensity/%
100
80
60
40
20
0
0
5
10
Time/min
220 nm
280 nm

9

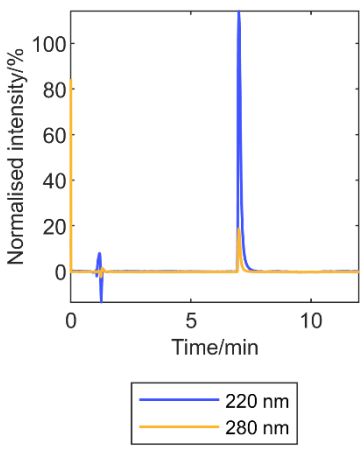
Normalised intensity/%
100
80
60
40
20
0
0
5
10
Time/min
220 nm
280 nm

10

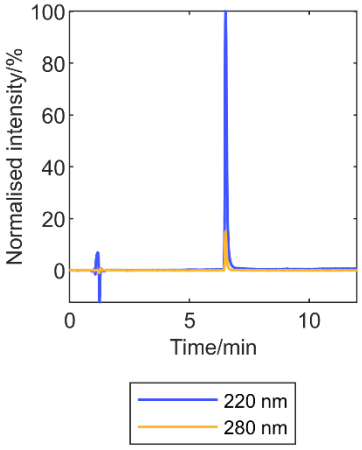
Normalised intensity/%
100
80
60
40
20
0
0
5
10
Time/min
220 nm
280 nm

11

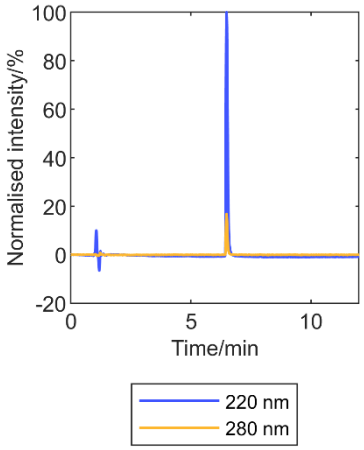
Normalised intensity/%
100
80
60
40
20
0
-20
0
5
10
Time/min
220 nm
280 nm

12

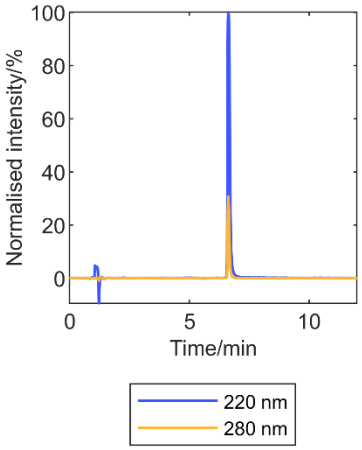
Normalised intensity/%
100
80
60
40
20
0
0
5
10
Time/min
220 nm
280 nm

13

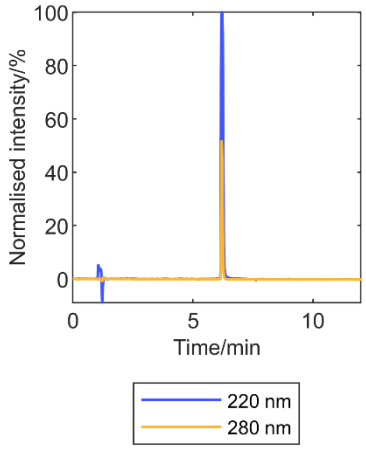

14

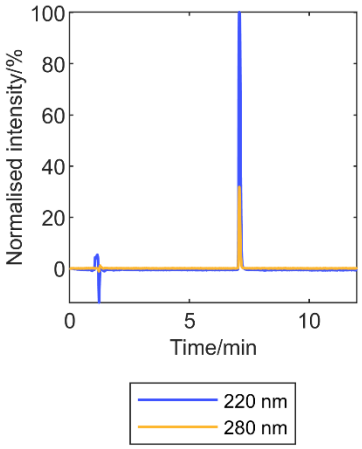

15

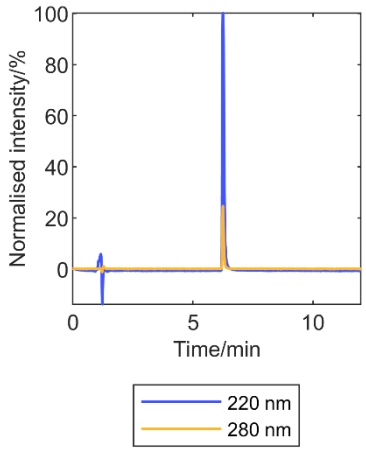

16

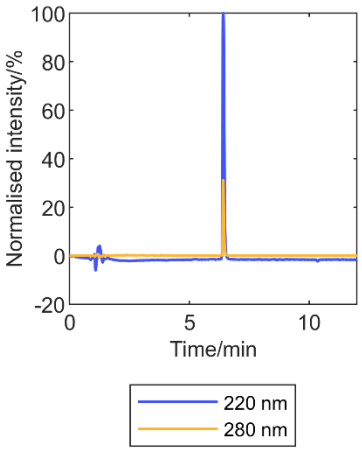

17

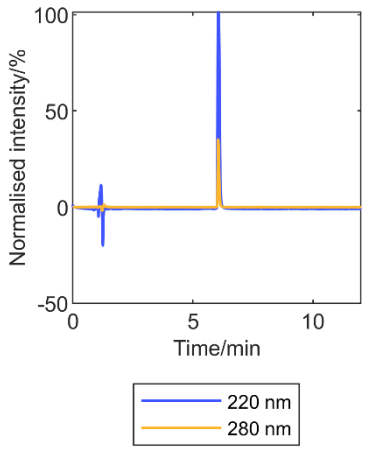

18

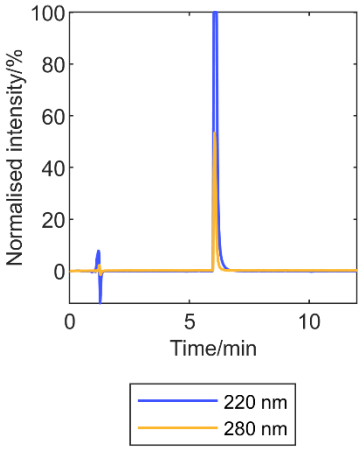

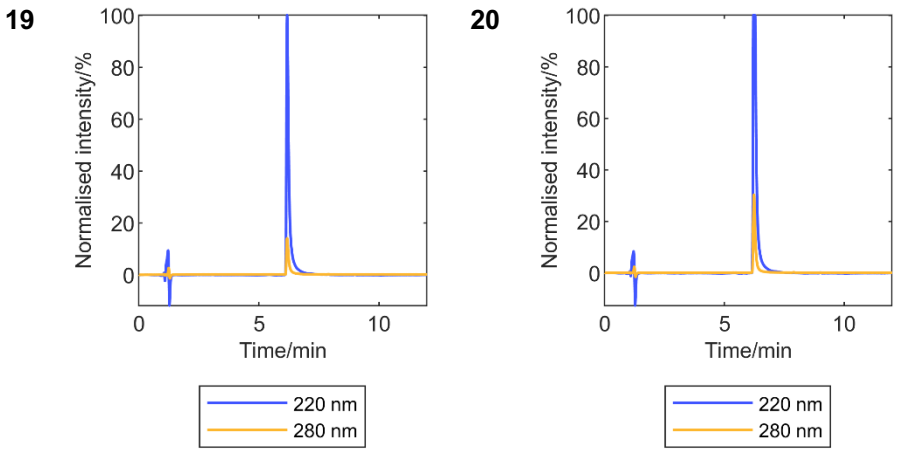

Figure S3 Representative analytical HPLC traces monitoring absorbance at 220 nm and 280 nm of all discussed peptides. Absorbances are reported as normalised intensities. Peptides numbered as in Table S1.

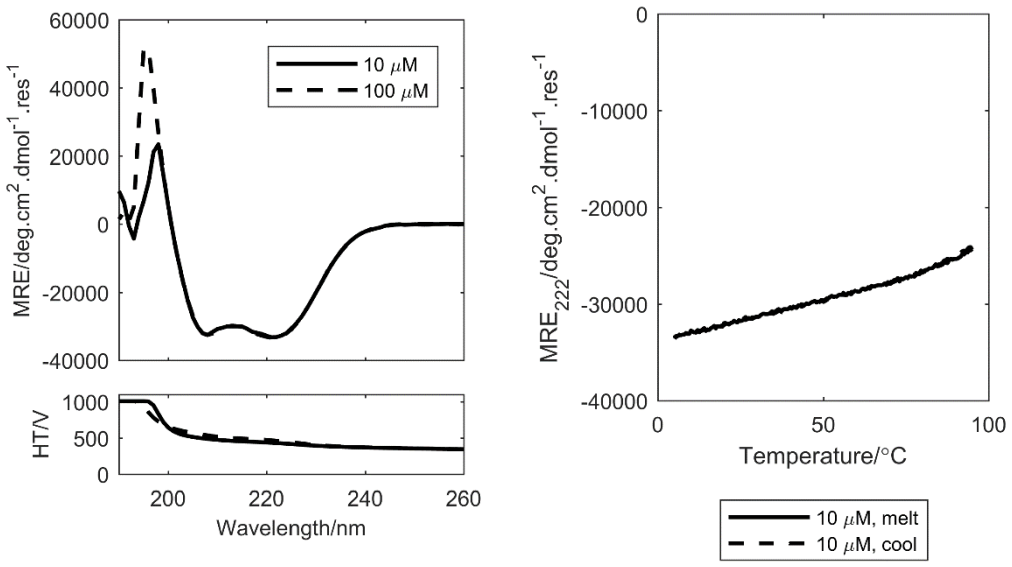

Figure S4 CD spectroscopy data for CC-Tet. Left: CD spectra (top) and high tension (HT) plots (bottom) at 10 and 100 μM. Right: Variable temperature (5–95–5 °C) measurement at 10 μM. All measurements were performed in PBS (pH 7.4).

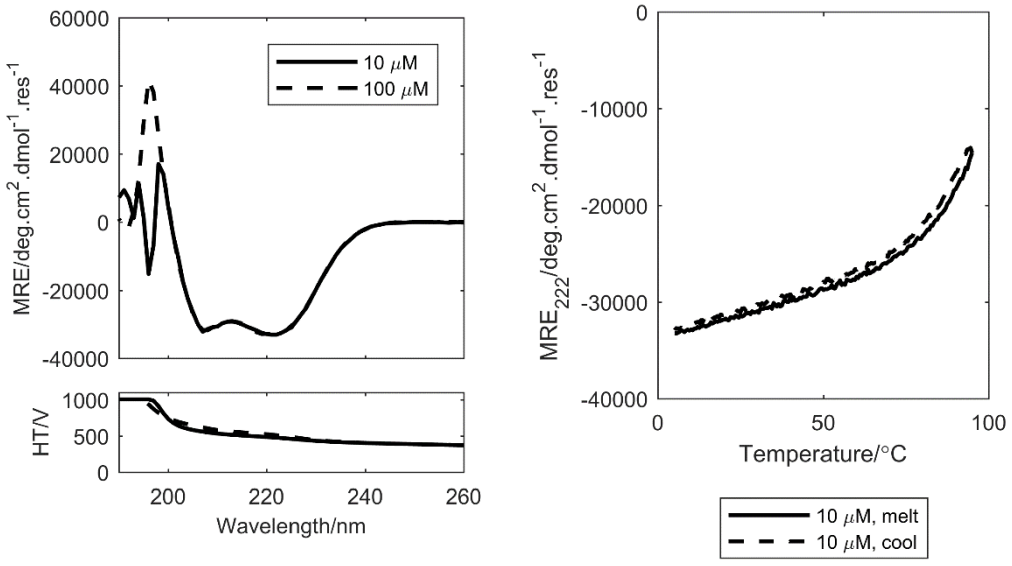

Figure S5 CD spectroscopy data for CC-Tet-KE. Left: CD spectra (top) and HT plots (bottom) at 10 and 100 μM. Right: Variable temperature (5–95–5 °C) measurement at 10 μM. All measurements were performed in PBS (pH 7.4).

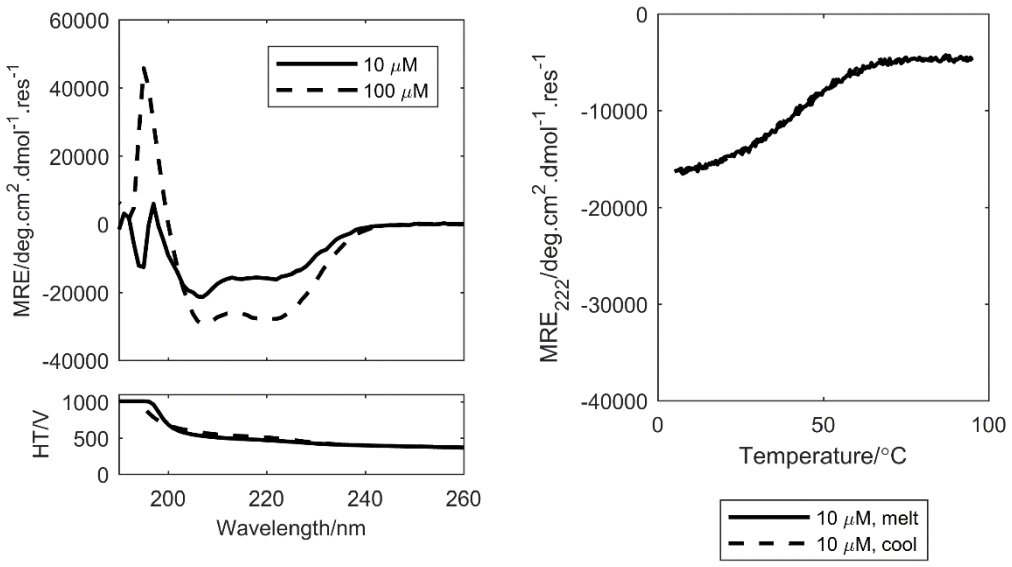

Figure S6 CD spectroscopy data for CC-Tet-3. Left: CD spectra (top) and HT plots (bottom) at 10 and 100 μM. Right: Variable temperature (5–95–5 °C) measurement at 10 μM. All measurements were performed in PBS (pH 7.4).

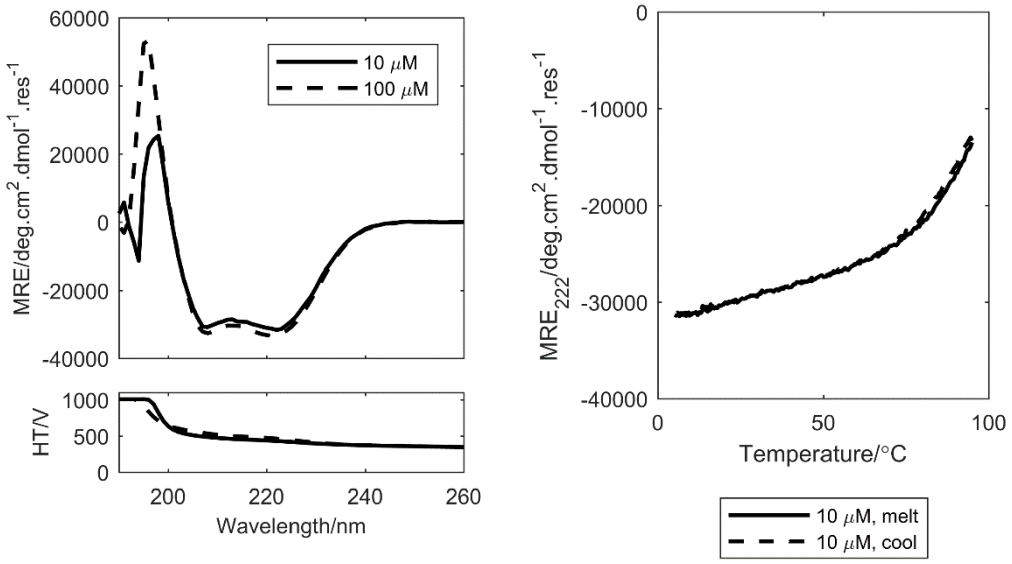

Figure S7 CD spectroscopy data for 1-EK-4. Left: CD spectra (top) and HT plots (bottom) at 10 and 100 μM. Right: Variable temperature (5–95–5 °C) measurement at 10 μM. All measurements were performed in PBS (pH 7.4).

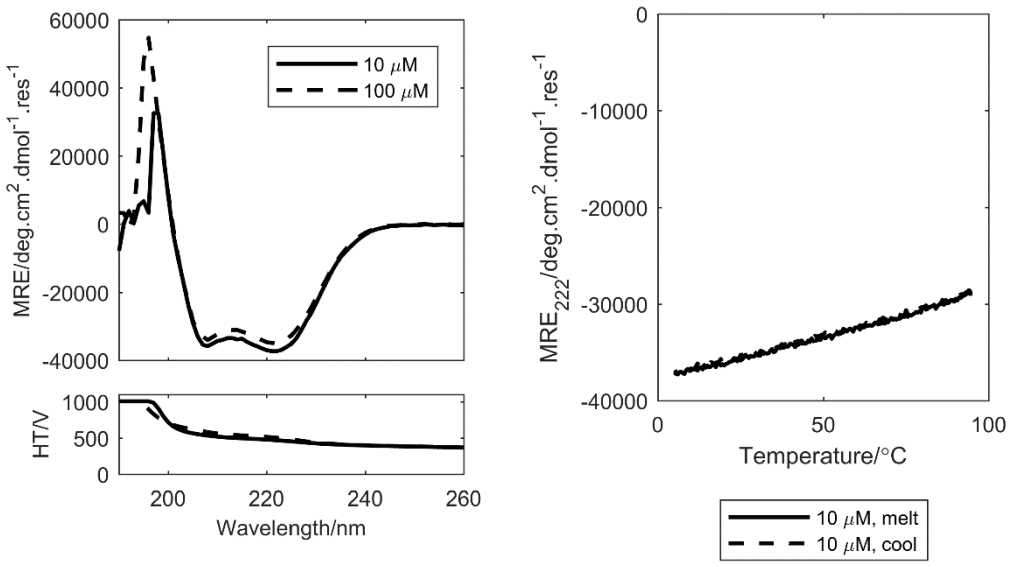

Figure S8 CD spectroscopy data for 1-KE-4. Left: CD spectra (top) and HT plots (bottom) at 10 and 100 μM. Right: Variable temperature (5–95–5 °C) measurement at 10 μM. All measurements were performed in PBS (pH 7.4).

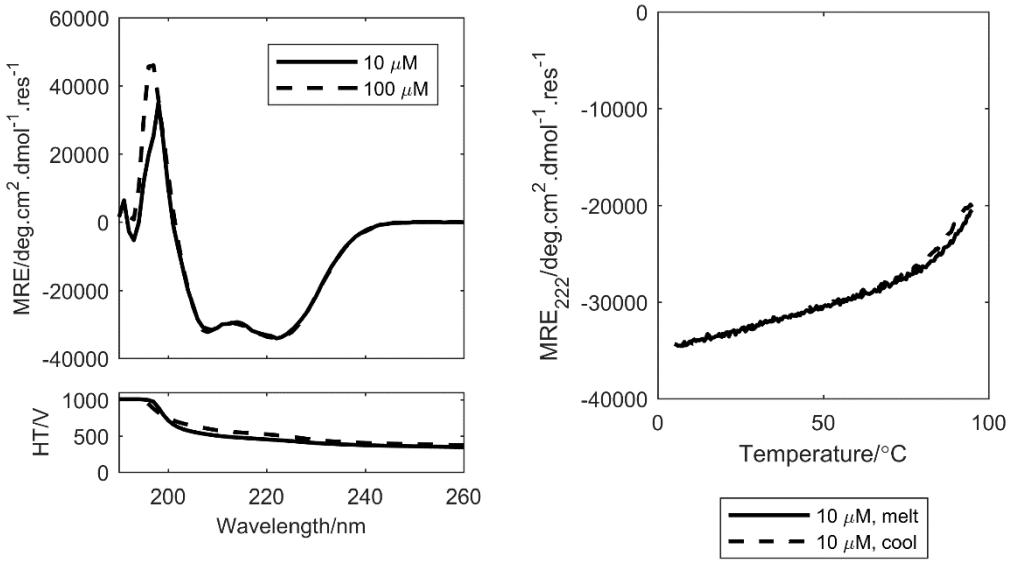

Figure S9 CD spectroscopy data for 2-EK-4. Left: CD spectra (top) and HT plots (bottom) at 10 and 100 μM. Right: Variable temperature (5–95–5 °C) measurement at 10 μM. All measurements were performed in PBS (pH 7.4).

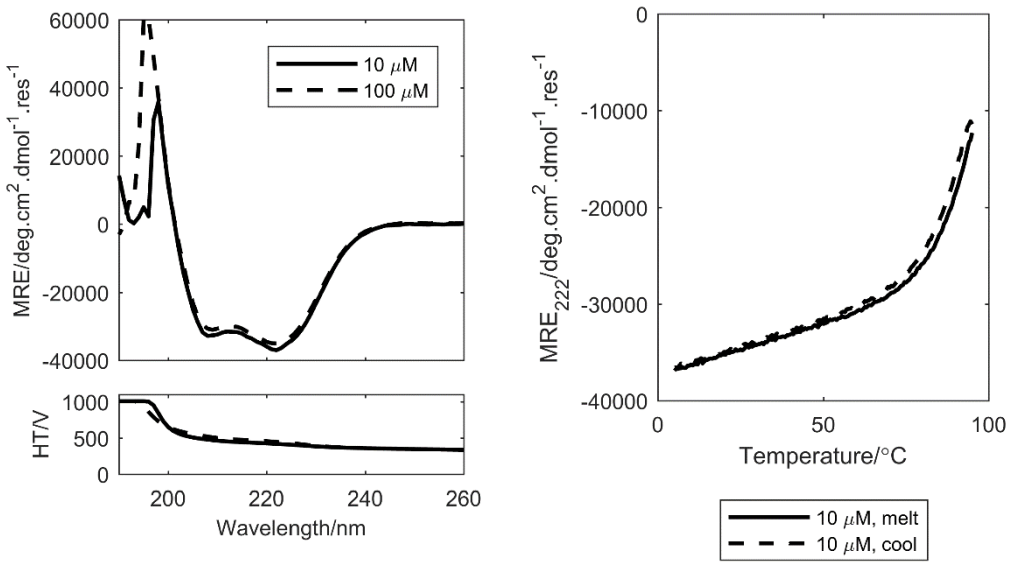

Figure S10 CD spectroscopy data for 2-KE-4. Left: CD spectra (top) and HT plots (bottom) at 10 and 100 μM. Right: Variable temperature (5–95–5 °C) measurement at 10 μM. All measurements were performed in PBS (pH 7.4).

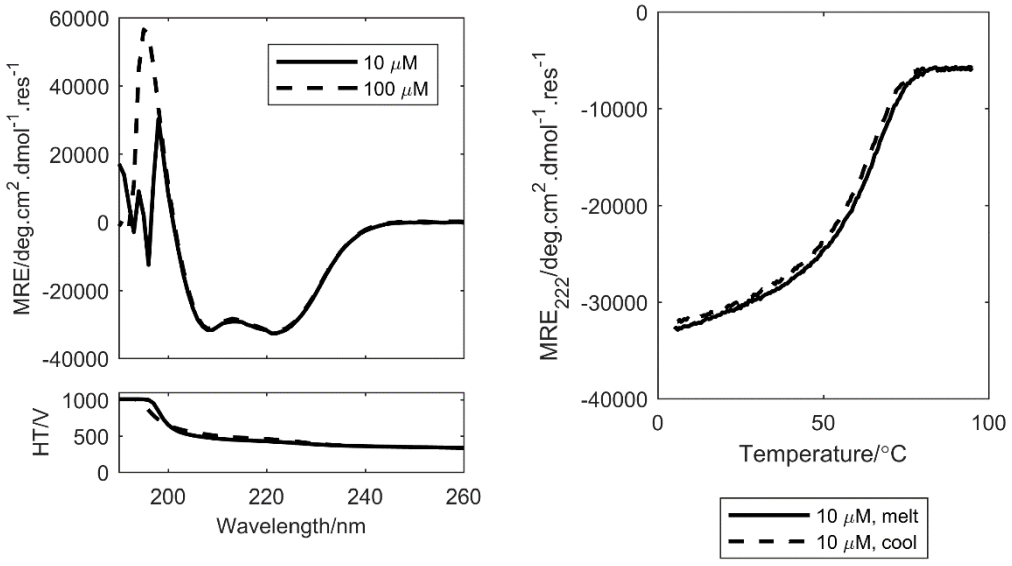

Figure S11 CD spectroscopy data for 3-EK-4. Left: CD spectra (top) and HT plots (bottom) at 10 and 100 μM. Right: Variable temperature (5–95–5 °C) measurement at 10 μM. All measurements were performed in PBS (pH 7.4).

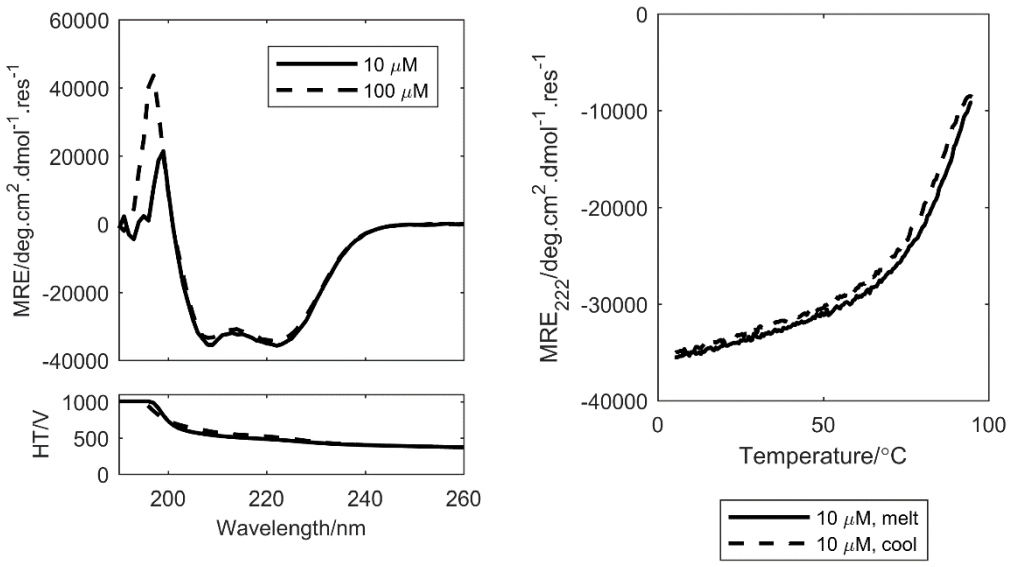

Figure S12 CD spectroscopy data for 3-KE-4. Left: CD spectra (top) and HT plots (bottom) at 10 and 100 μM. Right: Variable temperature (5–95–5 °C) measurement at 10 μM. All measurements were performed in PBS (pH 7.4).

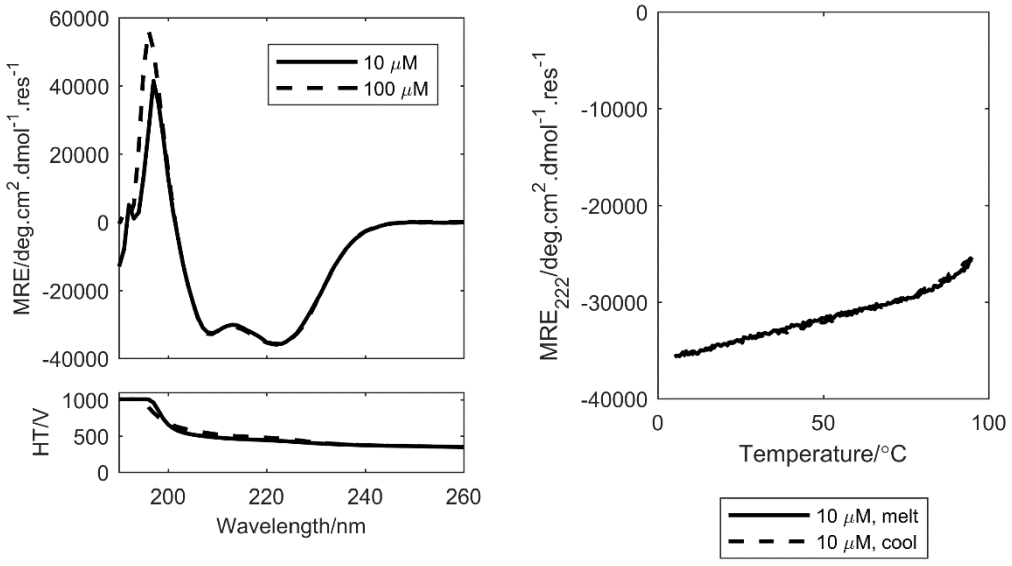

Figure S13 CD spectroscopy data for 4-EK-4. Left: CD spectra (top) and HT plots (bottom) at 10 and 100 μM. Right: Variable temperature (5–95–5 °C) measurement at 10 μM. All measurements were performed in PBS (pH 7.4).

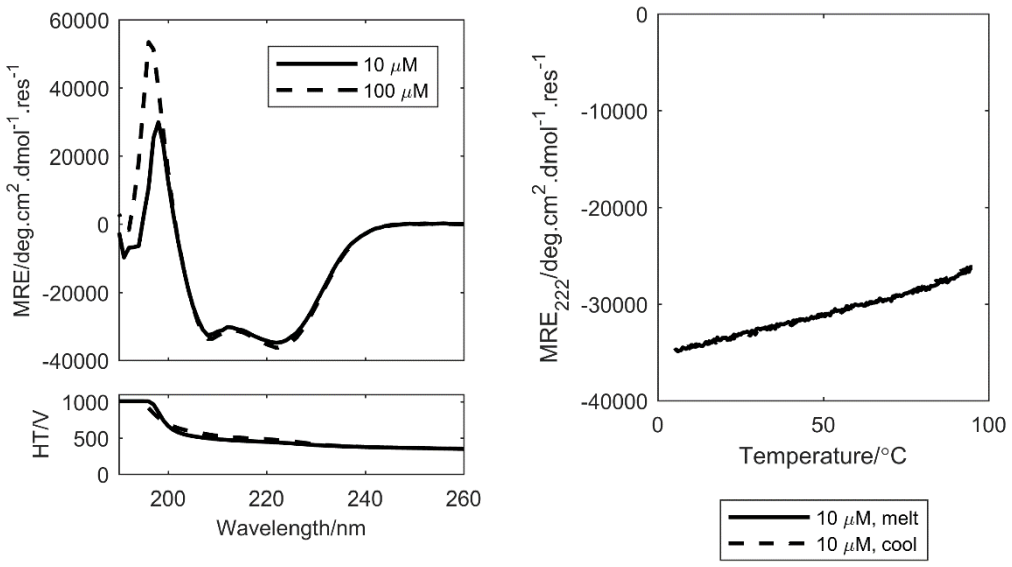

Figure S14 CD spectroscopy data for 4-KE-4. Left: CD spectra (top) and HT plots (bottom) at 10 and 100 μM. Right: Variable temperature (5–95–5 °C) measurement at 10 μM. All measurements were performed in PBS (pH 7.4).

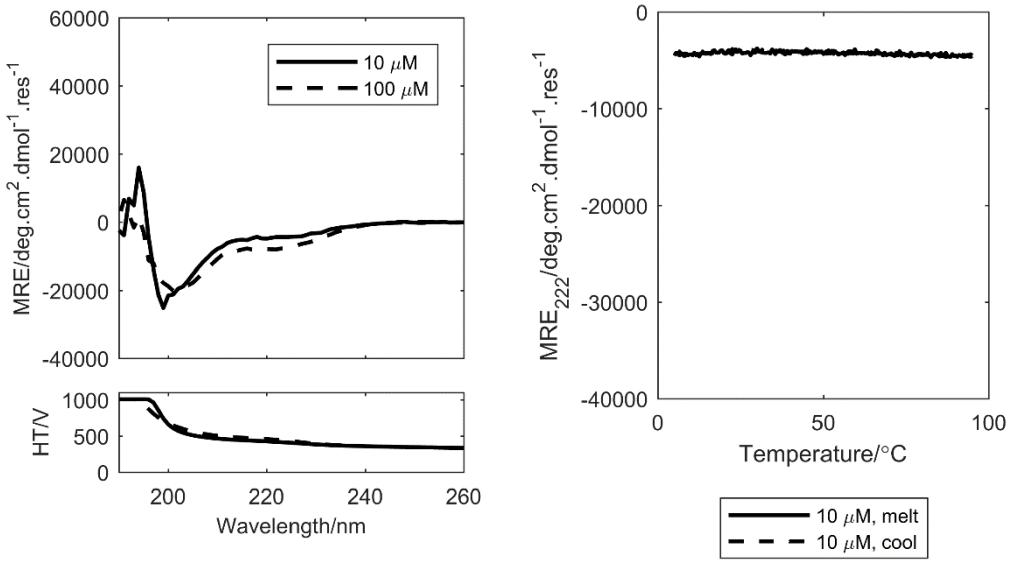

Figure S15 CD spectroscopy data for 1-EK-3. Left: CD spectra (top) and HT plots (bottom) at 10 and 100 μM. Right: Variable temperature (5–95–5 °C) measurement at 10 μM. All measurements were performed in PBS (pH 7.4).

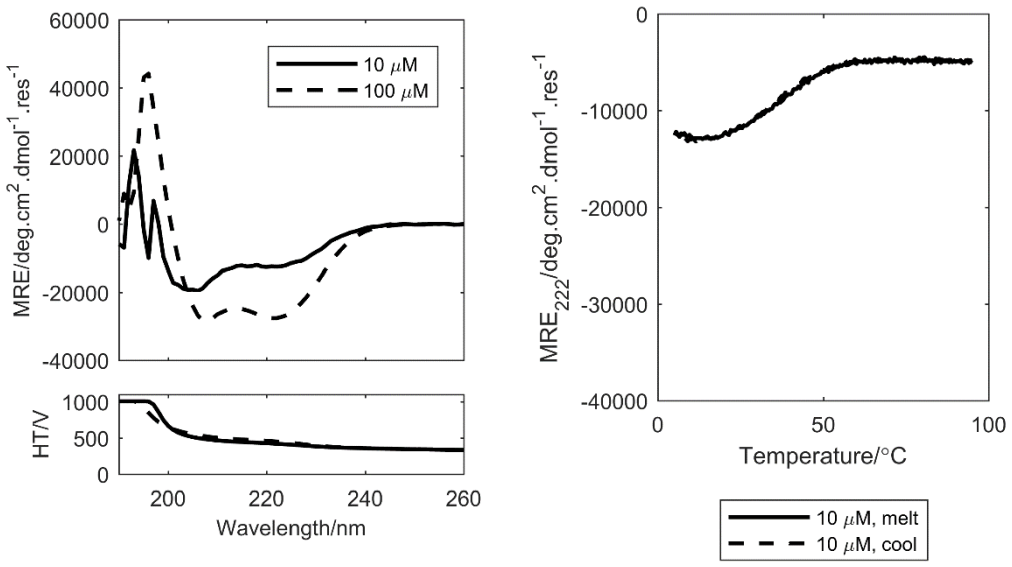

Figure S16 CD spectroscopy data for 2-EK-3. Left: CD spectra (top) and HT plots (bottom) at 10 and 100 μM. Right: Variable temperature (5–95–5 °C) measurement at 10 μM. All measurements were performed in PBS (pH 7.4).

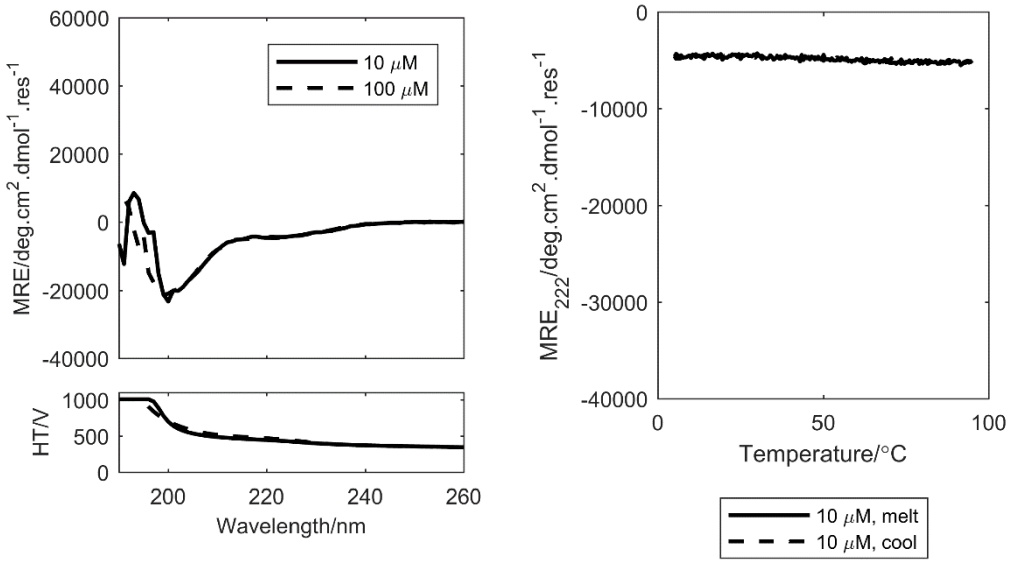

Figure S17 CD spectroscopy data for 3-EK-3. Left: CD spectra (top) and HT plots (bottom) at 10 and 100 μM. Right: Variable temperature (5–95–5 °C) measurement at 10 μM. All measurements were performed in PBS (pH 7.4).

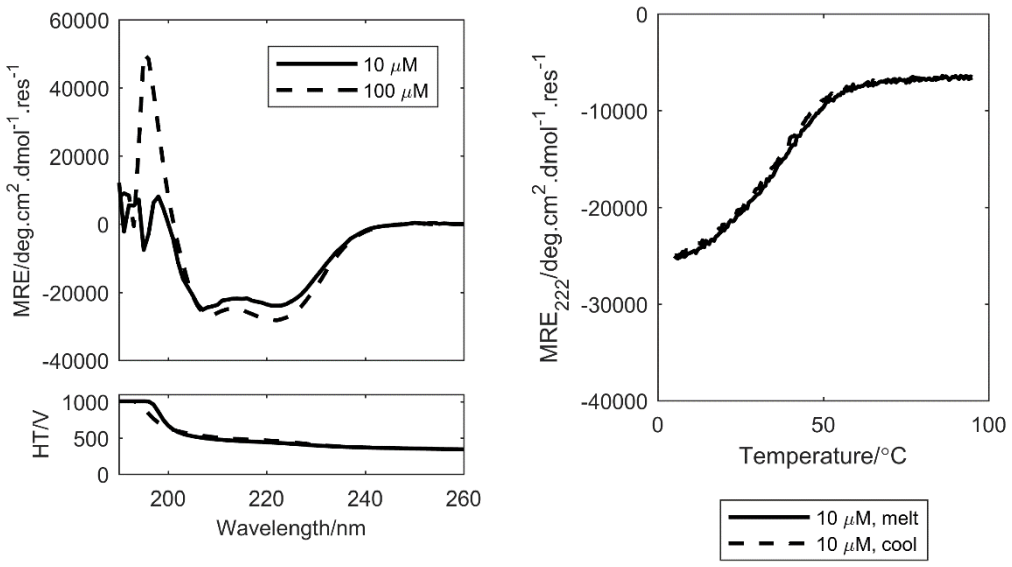

Figure S18 CD spectroscopy data for 4-EK-3. Left: CD spectra (top) and HT plots (bottom) at 10 and 100 μM. Right: Variable temperature (5–95–5 °C) measurement at 10 μM. All measurements were performed in PBS (pH 7.4).

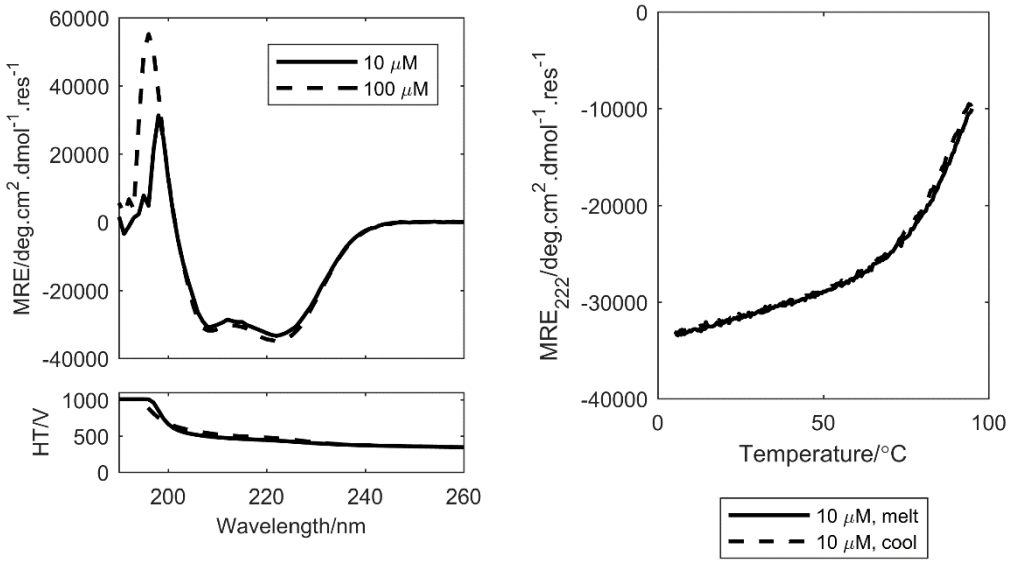

Figure S19 CD spectroscopy data for 4-EK-3.5-N. Left: CD spectra (top) and HT plots (bottom) at 10 and 100 μM. Right: Variable temperature (5–95–5 °C) measurement at 10 μM. All measurements were performed in PBS (pH 7.4).

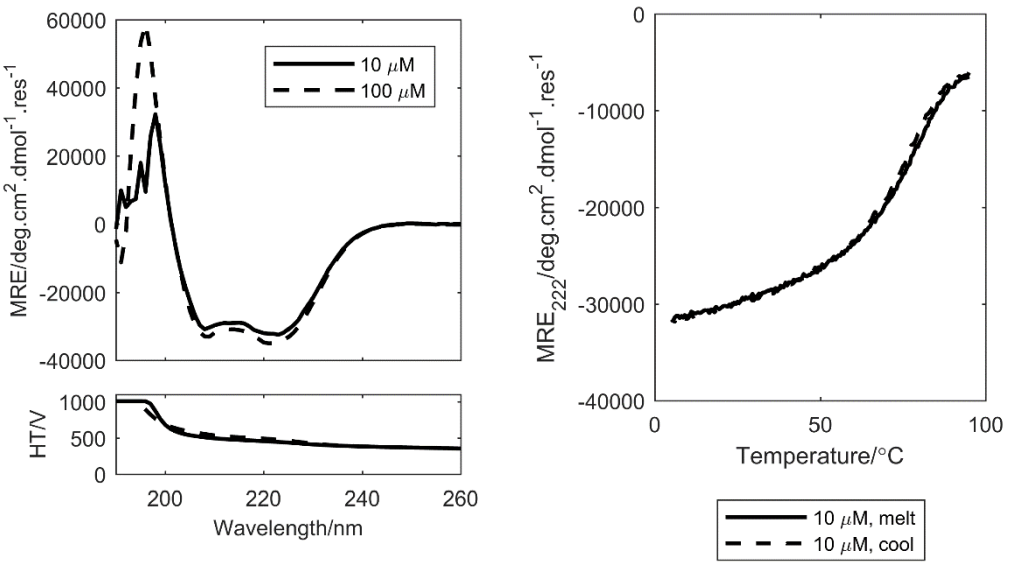

Figure S20 CD spectroscopy data for 4-EK-3.5-C. Left: CD spectra (top) and HT plots (bottom) at 10 and 100 μM. Right: Variable temperature (5–95–5 °C) measurement at 10 μM. All measurements were performed in PBS (pH 7.4).

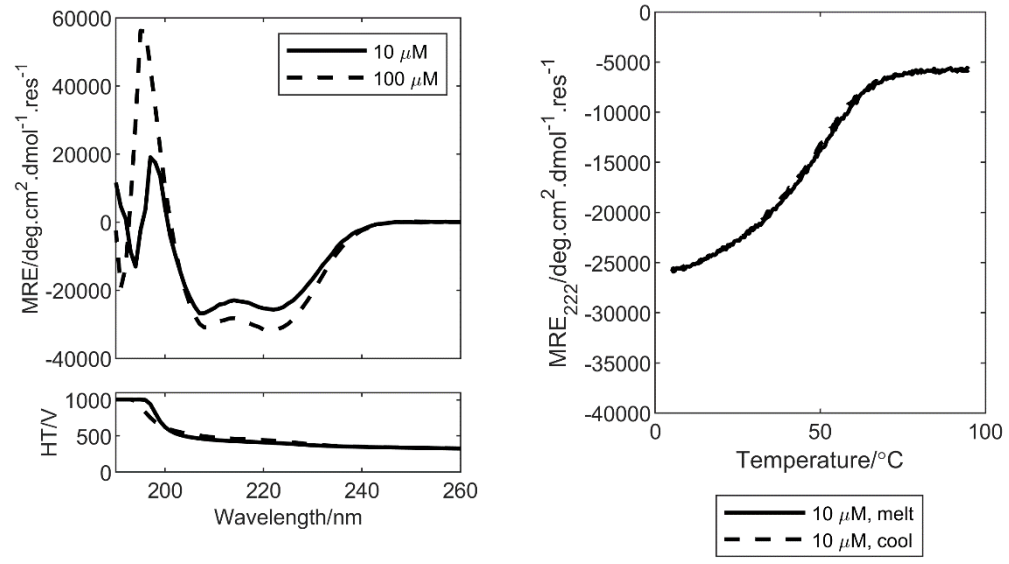

Figure S21 CD spectroscopy data for 4-KE-3. Left: CD spectra (top) and HT plots (bottom) at 10 and 100 μM. Right: Variable temperature (5–95–5 °C) measurement at 10 μM. All measurements were performed in PBS (pH 7.4).

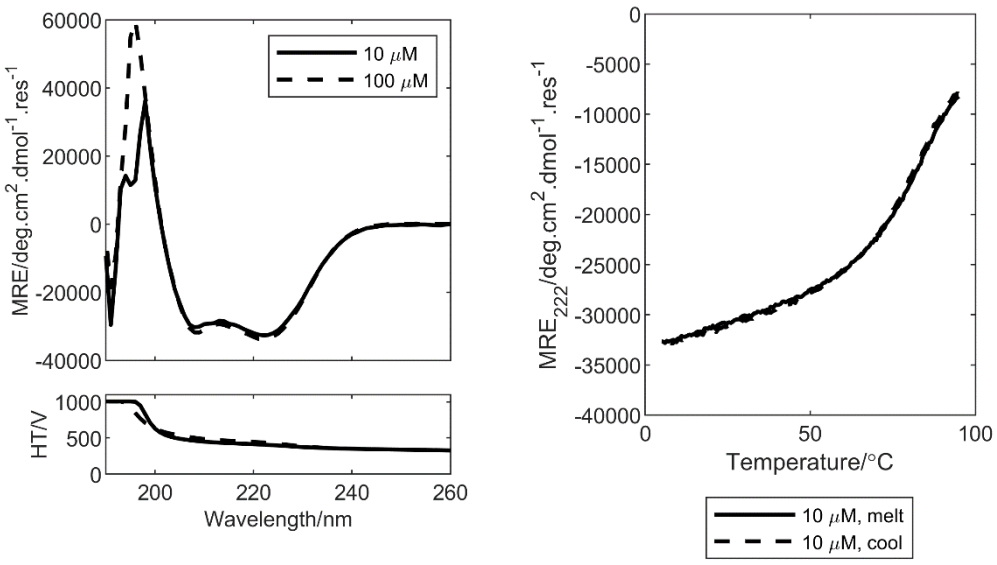

Figure S22 CD spectroscopy data for 4-KE-3.5-N. Left: CD spectra (top) and HT plots (bottom) at 10 and 100 μM. Right: Variable temperature (5–95–5 °C) measurement at 10 μM. All measurements were performed in PBS (pH 7.4).

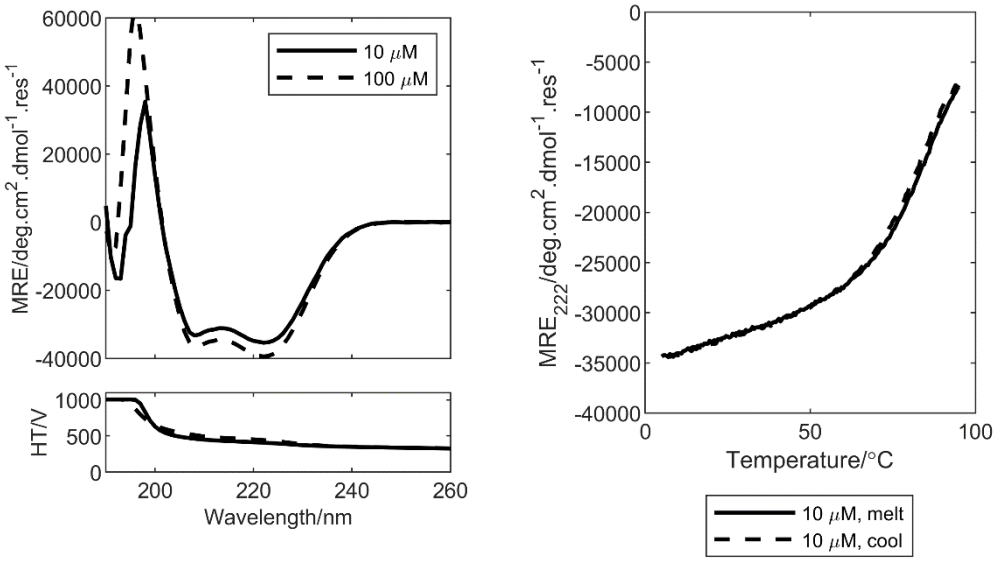

Figure S23 CD spectroscopy data for 4-KE-3.5-C. Left: CD spectra (top) and HT plots (bottom) at 10 and 100 μM. Right: Variable temperature (5–95–5 °C) measurement at 10 μM. All measurements were performed in PBS (pH 7.4).

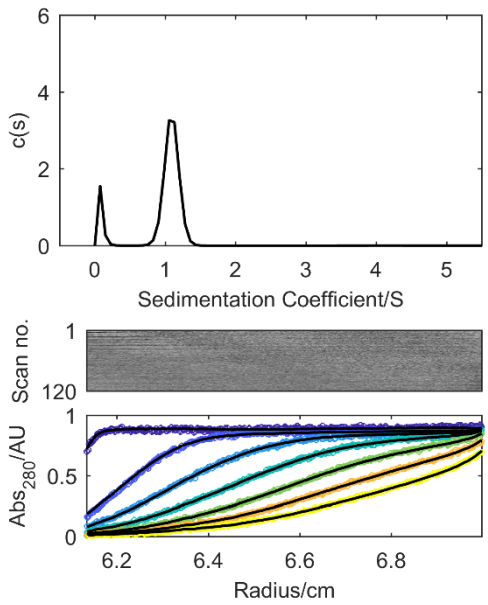

Figure S24 Sedimentation velocity (SV) data for CC-Tet ($\bar{v}$ = 0.7698 $cm^3.g^{-1}$). Continuous c(s) distribution fits (top), residuals (middle) and example data (circles) and fits (black lines) (bottom) at 50 krpm returning s = 1.09, $s_{20,w}$ = 1.12, f/f_0 = 1.31 and Mw = 10677 Da (3.16 x monomer mass).

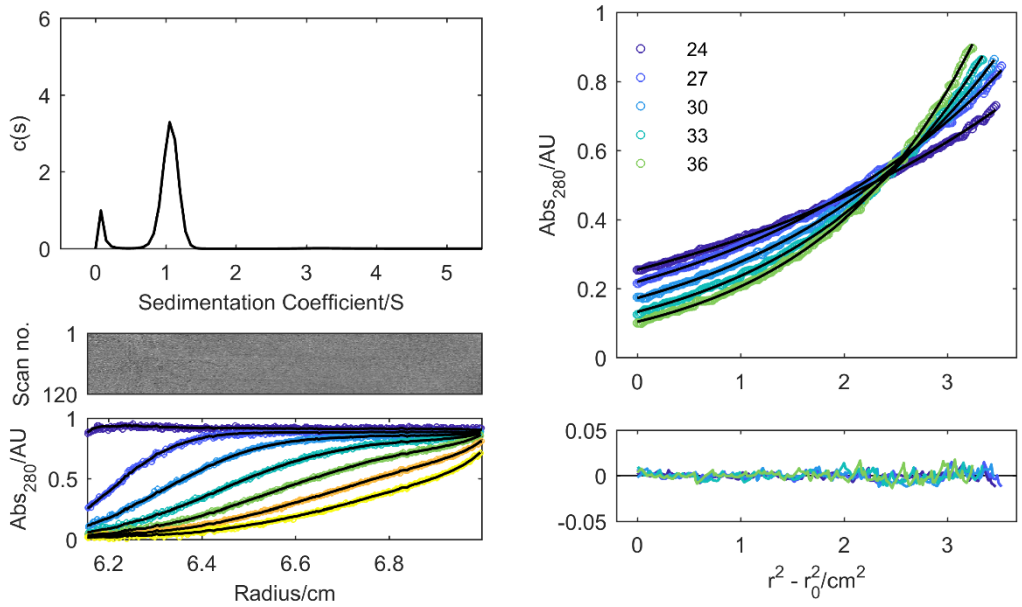

Figure S25 AUC data for CC-Tet-KE ($\bar{v}$ = 0.7696 $cm^3.g^{-1}$). Left: sedimentation velocity (SV) continuous c(s) distribution fits (top), residuals (middle) and example data (circles) and fits (black lines) (bottom) at 50 krpm returning s = 1.06, $s_{20,w}$ =1.09, f/f_0 = 1.33 and Mw = 10491 Da (3.11 x monomer mass). Right, top: Sedimentation equilibrium (SE) data (circles) fitted to single-ideal species model curves (black lines) at 24, 27, 30, 33 and 36 krpm, returning Mw = 9561 Da (2.83 x monomer mass, 99 % confidence limits: 9502–9619 Da). Right, bottom: residuals for the above fit, same colours.

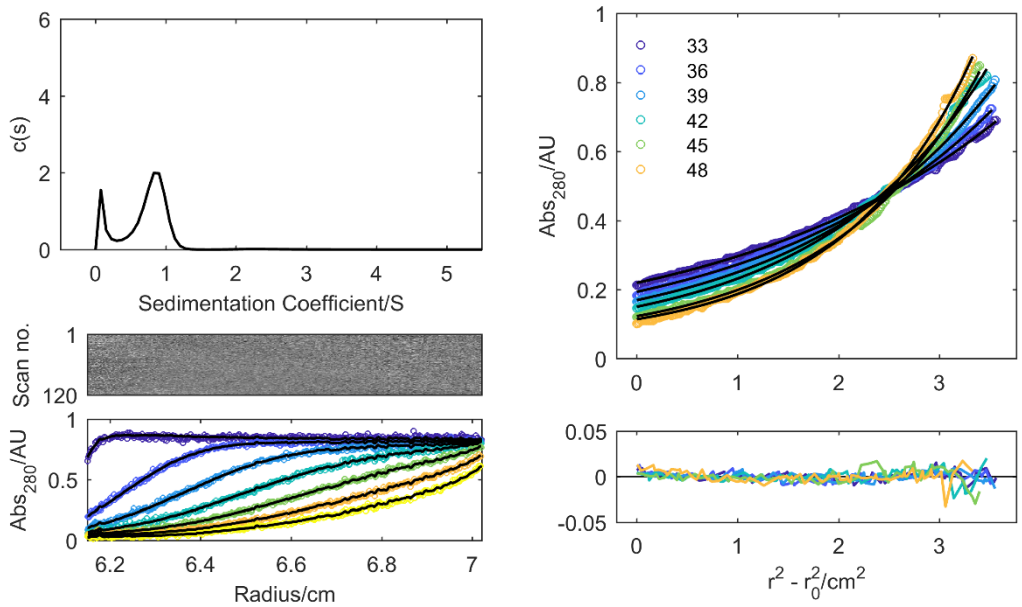

Figure S26 AUC data for CC-Tet-3 ($\bar{v}$ = 0.7725 $cm^3.g^{-1}$). Left: SV continuous c(s) distribution fits (top), residuals (middle) and example data (circles) and fits (black lines) (bottom) at 60 krpm returning s = 0.81, $s_{20,w}$ = 0.83, f/f_0 = 1.34 and Mw = 7170 Da (2.88 x monomer mass). Right, top: SE data (circles) fitted to single-ideal species model curves (black lines) at 30, 33, 36, 39, 42, 45 and 48 krpm, returning Mw = 6680 Da (2.68 x monomer mass, 99 % confidence limits: 6641–6719 Da). Right, bottom: residuals for the above fit, same colours.

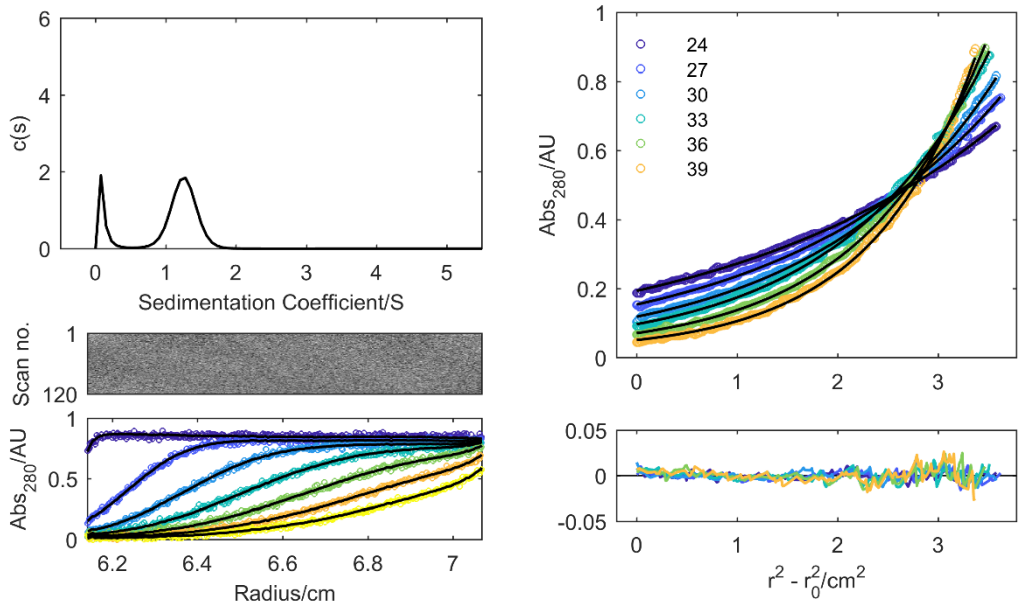

Figure S27 AUC data for 1-EK-4 ($\bar{v}$ = 0.7669 $cm^3.g^{-1}$). Left: SV continuous c(s) distribution fits (top), residuals (middle) and example data (circles) and fits (black lines) (bottom) at 50 krpm returning s = 1.25, $s_{20,w}$ = 1.28, f/f_0 = 1.32 and Mw = 12931 Da (3.98 x monomer mass). Right, top: SE data (circles) fitted to single-ideal species model curves (black lines) at 24, 27, 30, 33, 36 and 39 krpm, returning Mw = 12140 Da (3.74 x monomer mass, 99 % confidence limits: 12091–12186 Da). Right, bottom: residuals for the above fit, same colours.

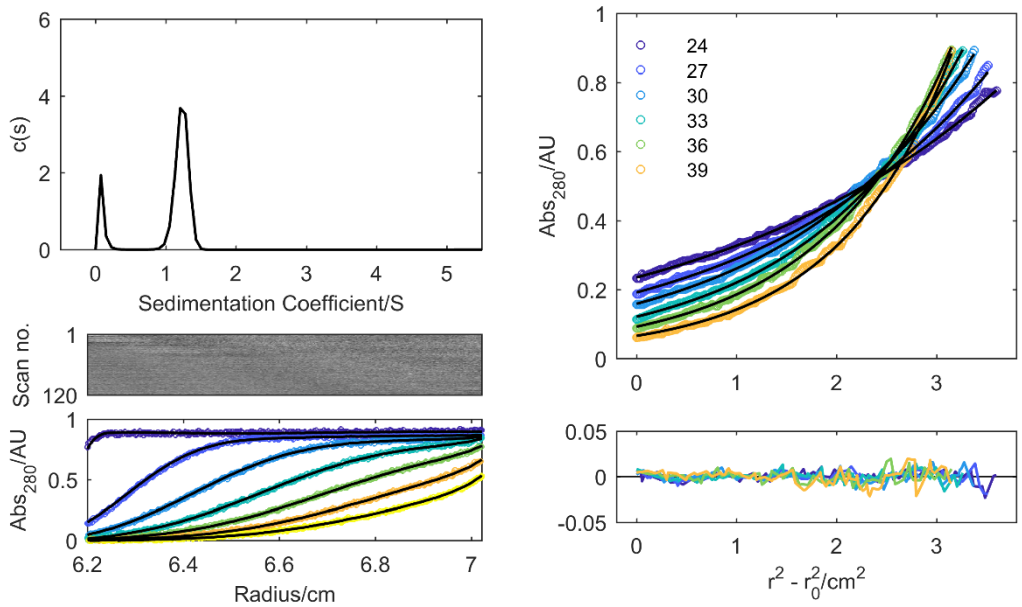

Figure S28 AUC data for 1-KE-4 ($\bar{v}$ = 0.7669 $cm^3.g^{-1}$). Left: SV continuous c(s) distribution fits (top), residuals (middle) and example data (circles) and fits (black lines) (bottom) at 50 krpm returning s = 1.23, $s_{20,w}$ = 1.26, f/f_0 = 1.23 and Mw = 11328 Da (3.49 x monomer mass). Right, top: SE data (circles) fitted to single-ideal species model curves (black lines) at 24, 27, 30, 33, 36 and 39 krpm, returning Mw = 11310 Da (3.48 x monomer mass, 99 % confidence limits: 11253–11361 Da). Right, bottom: residuals for the above fit, same colours.

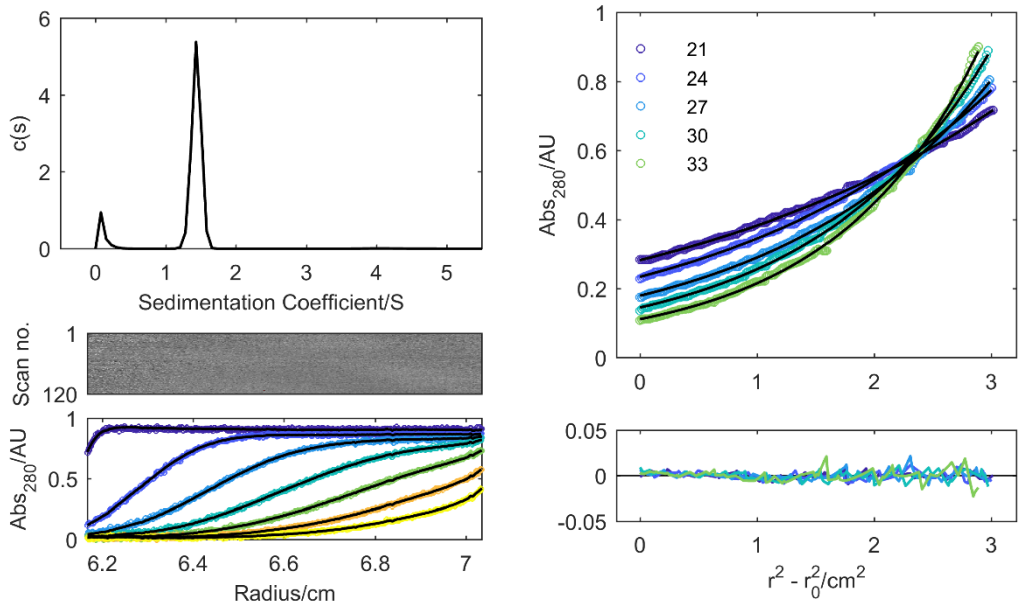

Figure S29 AUC data for 2-EK-4 ($\bar{v}$ = 0.7545 $cm^3.g^{-1}$). Left: SV continuous c(s) distribution fits (top), residuals (middle) and example data (circles) and fits (black lines) (bottom) at 50 krpm returning s = 1.44, $s_{20,w}$ = 1.47, f/f_0 = 1.25 and Mw = 13381 Da (3.85 x monomer mass). Right, top: SE data (circles) fitted to single-ideal species model curves (black lines) at 21, 24, 27, 30 and 33 krpm, returning Mw = 13600 Da (3.91 x monomer mass, 99 % confidence limits: 13506–13687 Da). Right, bottom: residuals for the above fit, same colours.

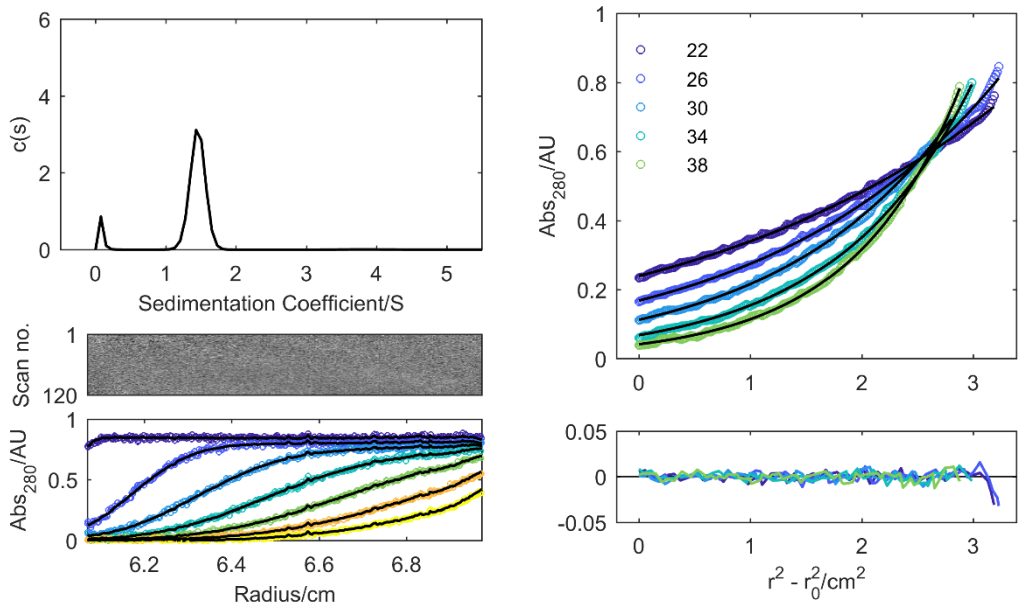

Figure S30 AUC data for 2-KE-4 ($\bar{v}$ = 0.7545 $cm^3.g^{-1}$). Left: SV continuous c(s) distribution fits (top), residuals (middle) and example data (circles) and fits (black lines) (bottom) at 50 krpm returning s = 1.46, $s_{20,w}$ = 1.49, f/f_0 = 1.29 and Mw = 14405 Da (4.15 x monomer mass). Right, top: SE data (circles) fitted to single-ideal species model curves (black lines) at 22, 26, 30, 34 and 38 krpm, returning Mw = 13150 Da (3.78 x monomer mass, 99 % confidence limits: 13092–13182 Da). Right, bottom: residuals for the above fit, same colours.

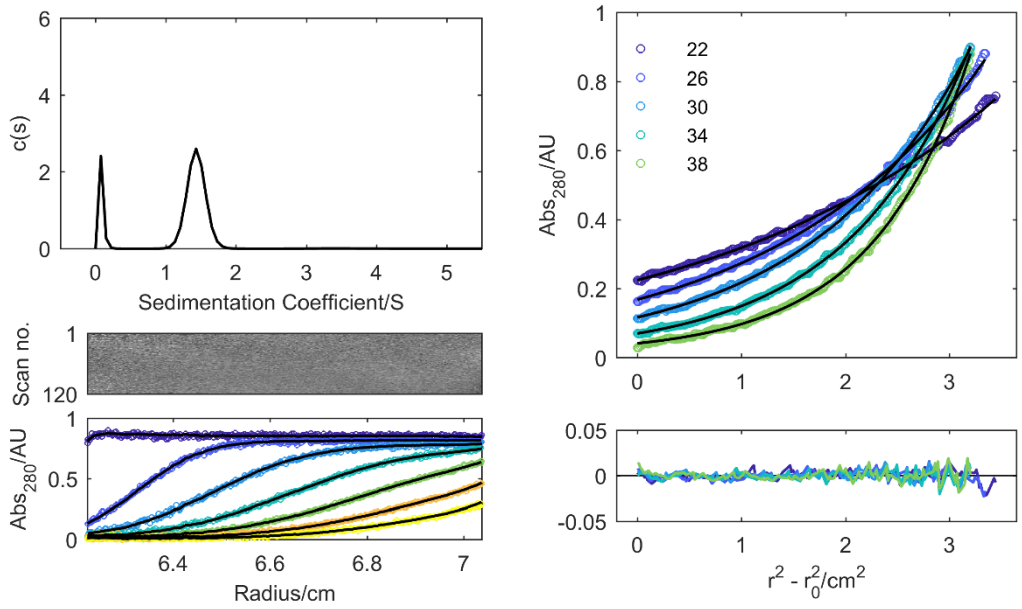

Figure S31 AUC data for 3-EK-4 ($\bar{v}$ = 0.7545 $cm^3.g^{-1}$). Left: SV continuous c(s) distribution fits (top), residuals (middle) and example data (circles) and fits (black lines) (bottom) at 50 krpm returning s = 1.43, $s_{20,w}$ = 1.47, f/f_0 = 1.32 and Mw = 14523 Da (4.18 x monomer mass). Right, top: SE data (circles) fitted to single-ideal species model curves (black lines) at 22, 26, 30, 34 and 38 krpm, returning Mw = 13420 Da (3.86 x monomer mass, 99 % confidence limits: 13338–13437 Da). Right, bottom: residuals for the above fit, same colours.

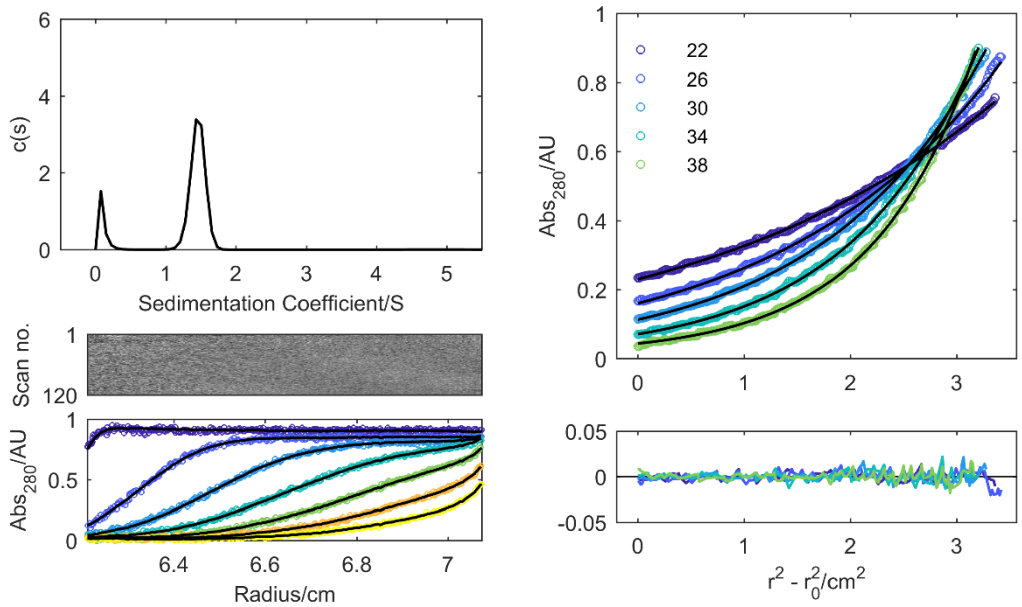

Figure S32 AUC data for 3-KE-4 ($\bar{v}$ = 0.7545 $cm^3.g^{-1}$). Left: SV continuous c(s) distribution fits (top), residuals (middle) and example data (circles) and fits (black lines) bottom) at 50 krpm returning s = 1.46, $s_{20,w}$ = 1.49, f/f_0 = 1.21 and Mw = 13119 Da (3.78 x monomer mass). Right, top: SE data (circles) fitted to single-ideal species model curves (black lines) at 22, 26, 30, 34 and 38 krpm, returning Mw = 13220 Da (3.80 x monomer mass, 99 % confidence limits: 13190–13284 Da). Right, bottom: residuals for the above fit, same colours.

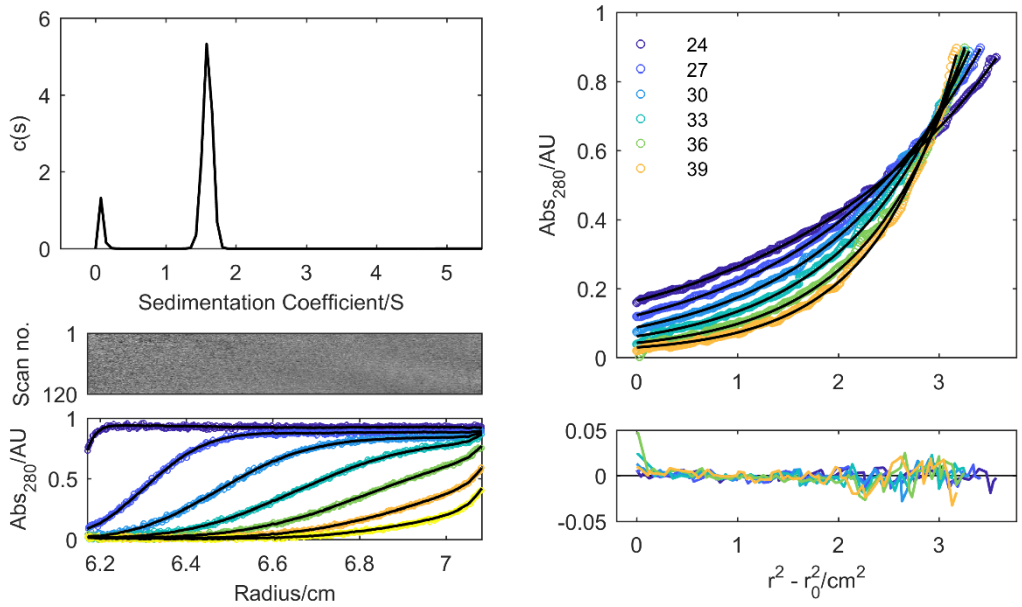

Figure S33 AUC data for 4-EK-4 ($\bar{v}$ = 0.7594 $cm^3.g^{-1}$). Left: SV continuous c(s) distribution fits (top), residuals (middle) and example data (circles) and fits (black lines) (bottom) at 50 krpm returning s = 1.60, $s_{20,w}$ = 1.63, f/f_0 = 1.20 and Mw = 15289 Da (4.13 x monomer mass). Right, top: SE data (circles) fitted to single-ideal species model curves (black lines) at 24, 27, 30, 33, 36 and 39 krpm, returning Mw = 15040 Da (4.06 x monomer mass, 99 % confidence limits: 14990–15099 Da). Right, bottom: residuals for the above fit, same colours.

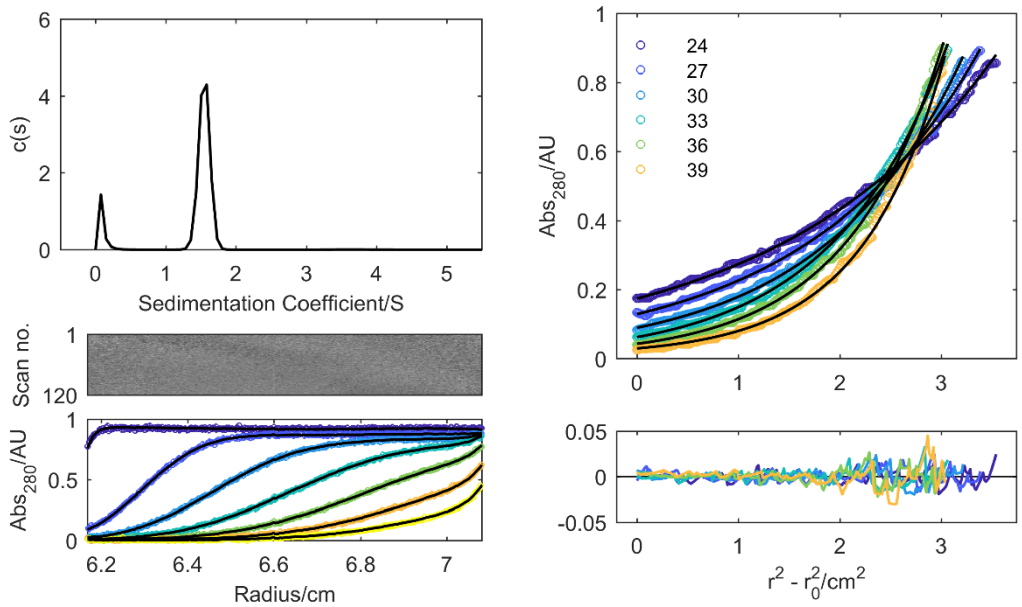

Figure S34 AUC data for 4-KE-4 ($\bar{v}$ = 0.7594 $cm^3.g^{-1}$). Left: SV continuous c(s) distribution fits (top), residuals (middle) and example data (circles) and fits (black lines) (bottom) at 50 krpm returning s = 1.55, $s_{20,w}$ = 1.59, f/f_0 = 1.24 and Mw = 15433 Da (4.17 x monomer mass). Right, top: SE data (circles) fitted to single-ideal species model curves (black lines) at 24, 27, 30, 33, 36 and 39 krpm, returning Mw = 15140 Da (4.09 x monomer mass, 99 % confidence limits: 15074–15200 Da). Right, bottom: residuals for the above fit, same colours.

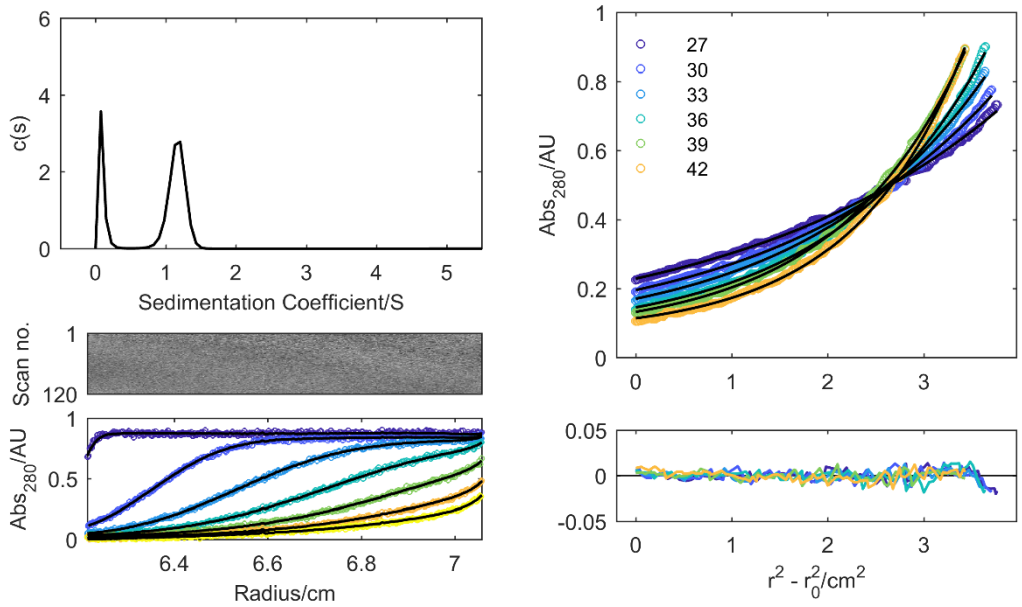

Figure S35 AUC data for 2-EK-3 ($\bar{v}$ = 0.7527 $cm^3.g^{-1}$). Left: SV continuous c(s) distribution fits (top), residuals (middle) and example data (circles) and fits (black lines) (bottom) at 60 krpm returning s = 1.16, $s_{20,w}$ = 1.19, f/f_0 = 1.20 and Mw = 9047 Da (3.40 x monomer mass). Right, top: SE data (circles) fitted to single-ideal species model curves (black lines) at 27, 30, 33, 36, 39 and 42 krpm, returning Mw = 8918 Da (3.35 x monomer mass, 99 % confidence limits: 8878–8957 Da). Right, bottom: residuals for the above fit, same colours.

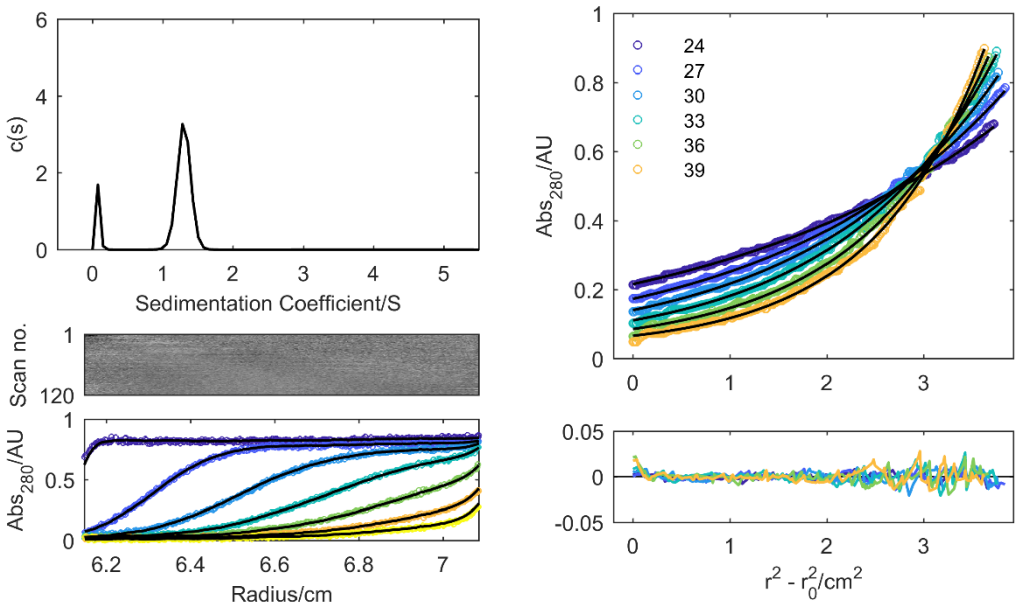

Figure S36 AUC data for 4-EK-3 ($\bar{v}$ = 0.7559 $cm^3.g^{-1}$). Left: SV continuous c(s) distribution fits (top), residuals (middle) and example data (circles) and fits (black lines) (bottom) at 60 krpm returning s = 1.30, $s_{20,w}$ = 1.33, f/f_0 = 1.22 and Mw = 11322 Da (3.99 x monomer mass). Right, top: SE data (circles) fitted to single-ideal species model curves (black lines) at 24, 27, 30, 33, 36 and 39 krpm, returning Mw = 10613 Da (3.74 x monomer mass, 99 % confidence limits: 10574–10652 Da). Right, bottom: residuals for the above fit, same colours.

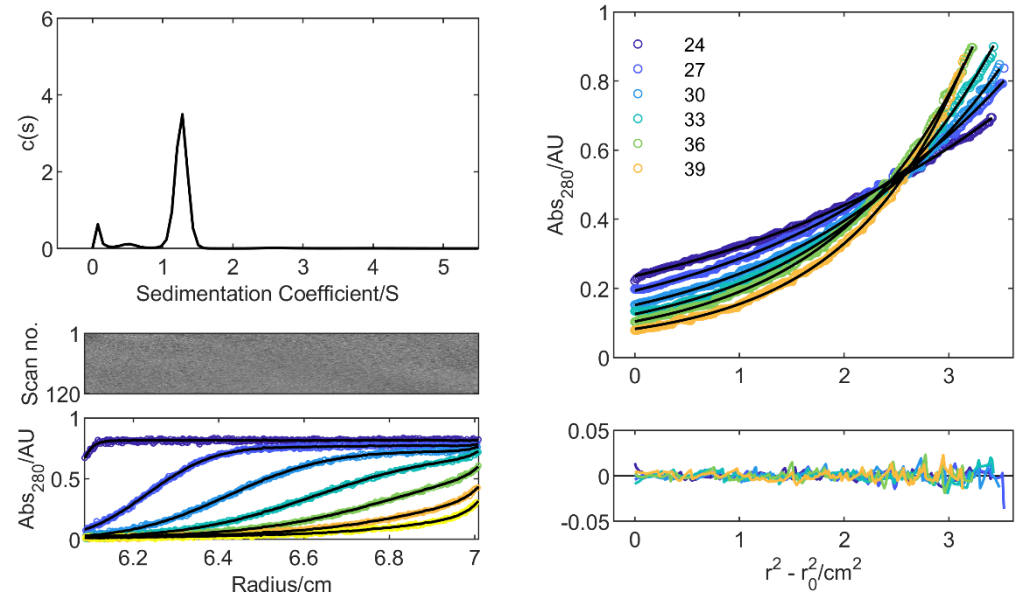

Figure S37 AUC data for 4-KE-3 ($\bar{v}$ = 0.7559 $cm^3.g^{-1}$). Left: SV continuous c(s) distribution fits (top), residuals (middle) and example data (circles) and fits (black lines) (bottom) at 60 krpm returning s = 1.265, $s_{20,w}$ = 1.293, f/f_0 = 1.21 and Mw = 10691 Da (3.77 x monomer mass). Right, top: SE data (circles) fitted to single-ideal species model curves (black lines) at 24, 27, 30, 33, 36 and 39 krpm, returning Mw = 10754 Da (3.79 x monomer mass, 99 % confidence limits: 10707–10800 Da). Right, bottom: residuals for the above fit, same colours.

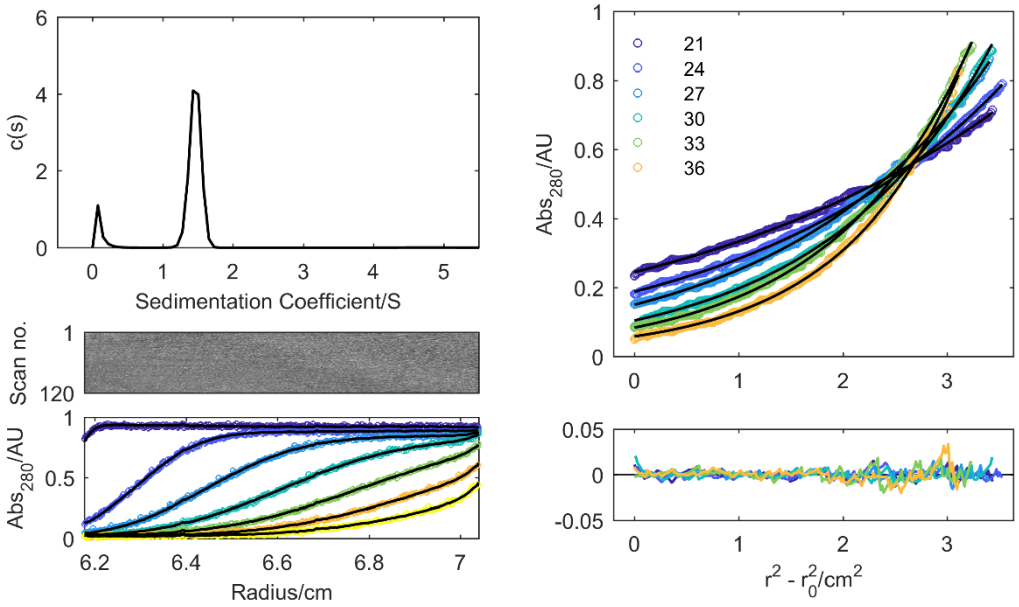

Figure S38 AUC data for 4-EK-3.5-C ($\bar{v}$ = 0.7622 $cm^3.g^{-1}$). Left: SV continuous c(s) distribution fits (top), residuals (middle) and example data (circles) and fits (black lines) (bottom) at 50 krpm returning s = 1.463, $s_{20,w}$ = 1.497, f/f_0 = 1.25 and Mw = 14031 Da (4.21 x monomer mass). Right, top: SE data (circles) fitted to single-ideal species model curves (black lines) at 21, 24, 27, 30, 33 and 36 krpm, returning Mw = 13102 Da (3.93 x monomer mass, 99 % confidence limits: 13053–13151 Da). Right, bottom: residuals for the above fit, same colours.

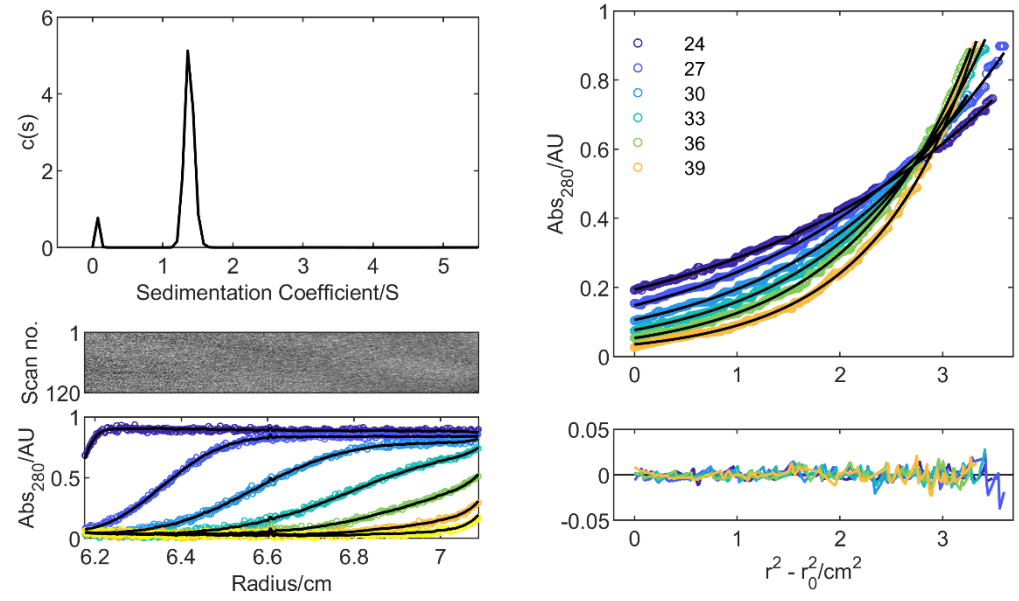

Figure S39 AUC data for 4-KE-3.5-N ($\bar{v}$ = 0.7599 $cm^3.g^{-1}$). Left: SV continuous c(s) distribution fits (top), residuals (middle) and example data (circles) and fits (black lines) (bottom) at 60 krpm returning s = 1.379, $s_{20,w}$ = 1.411, f/f_0 = 1.26 and Mw = 13222 Da (4.13 x monomer mass). Right, top: SE data (circles) fitted to single-ideal species model curves (black lines) at 24, 27, 30, 33, 36 and 39 krpm, returning Mw = 12527 Da (3.91 x monomer mass, 99 % confidence limits: 12490–12563 Da). Right, bottom: residuals for the above fit, same colours.

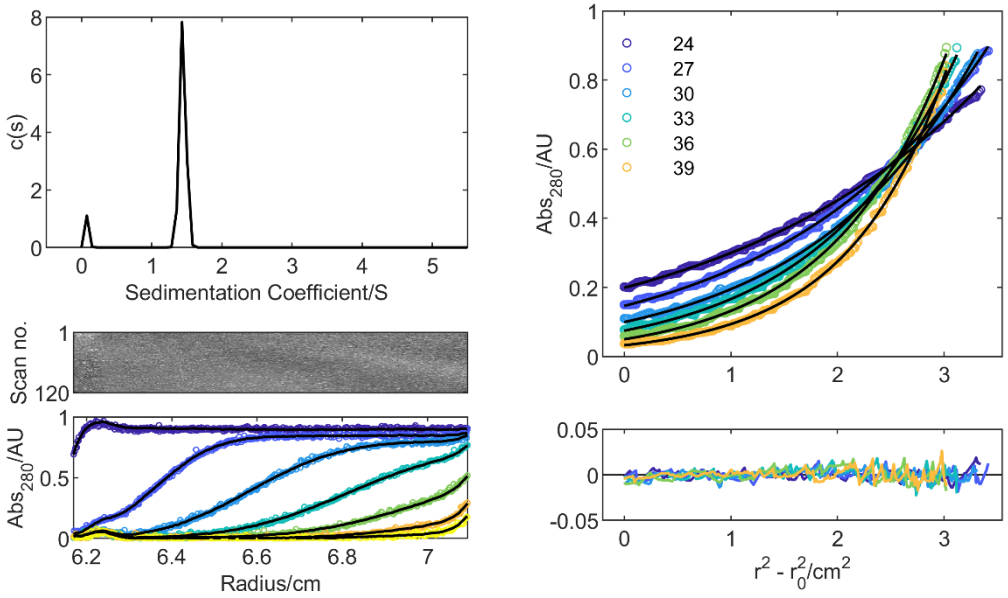

Figure S40 AUC data for 4-KE-3.5-C ($\bar{v}$ = 0.7559 $cm^3.g^{-1}$). Left: SV continuous c(s) distribution fits (top), residuals (middle) and example data (circles) and fits (black lines) (bottom) at 60 krpm returning s = 1.443, $s_{20,w}$ = 1.476, f/f_0 = 1.21 and Mw = 13100 Da (3.93 x monomer mass). Right, top: SE data (circles) fitted to single-ideal species model curves (black lines) at 24, 27, 30, 33, 36 and 39 krpm, returning Mw = 13181 Da (3.95 x monomer mass, 99 % confidence limits: 13141–13221 Da). Right, bottom: residuals for the above fit, same colours.

No.	Peptide	Sequence	Register	Heptad (*gabcde*)	Mass (Da)
1	CC-Tet	Ac – G E LAAIKQE LAAIKKE LAAIKWE LAAIKQ GAG – NH_2	*g*	ELAAIK	3374.993
2	CC-Tet-KE	Ac – G K LAAIEQK LAAIEKK LAAIEWK LAAIEQ GAG – NH_2	*g*	KLAAIE	3374.993
3	CC-Tet-3	Ac – G E LAAIKKE LAAIKWE LAAIKQ G – NH_2	*g*	ELAAIK	2492.967
4	1-EK-4	Ac – G AIKKE LAAIKKE LAAIKWE LAAIKKE LA G – NH_2	*c*	ELAAIK	3246.950
5	1-KE-4	Ac – G AIEQK LAAIEQK LAAIEWK LAAIEQK LA G – NH_2	*c*	KLAAIE	3246.820
6	2-EK-4	Ac – G EIKQQ LAEIKQQ LAEIKWQ LAEIKQQ LA G – NH_2	*c*	QLAEIK	3475.027
7	2-KE-4	Ac – G KIEQQ LAKIEQQ LAKIEWQ LAKIEQQ LA G – NH_2	*c*	QLAKIE	3475.027
8	3-EK-4	Ac – G AIQQE LKAIQQE LKAIQWE LKAIQQE LK G – NH_2	*c*	ELKAIQ	3475.027
9	3-KE-4	Ac – G AIQQK LEAIQQK LEAIQWK LEAIQQK LE G – NH_2	*c*	KLEAIQ	3475.027
10	4-EK-4	Ac – G KIQKQ LEKIQKQ LEKIQWQ LEKIQKQ LE G – NH_2	*c*	QLEKIQ	3703.364
11	4-KE-4	Ac – G EIQKQ LKEIQKQ LKEIQWQ LKEIQKQ LK G – NH_2	*c*	QLKEIQ	3703.364
12	1-EK-3	Ac – G AIKKE LAAIKWE LAAIKKE LA G – NH_2	*c*	ELAAIK	2493.011
13	2-EK-3	Ac – G EIKQQ LAEIKWQ LAEIKQQ LA G – NH_2	*c*	QLAEIK	2664.080
14	3-EK-3	Ac – G AIQQE LKAIQWE LKAIQQE LK G – NH_2	*c*	ELKAIQ	2664.080
15	4-EK-3	Ac – G KIQKQ LEKIQWQ LEKIQKQ LE G – NH_2	*c*	QLEKIQ	2835.322
16	4-EK-3.5-N	Ac – G Q LEKIQKQ LEKIQWQ LEKIQKQ LE G – NH_2	*g*	QLEKIQ	3205.727
17	4-EK-3.5-C	Ac – G KIQKQ LEKIQKQ LEKIQWQ LEKIQK G – NH_2	*c*	QLEKIQ	3332.959
18	4-KE-3	Ac – G EIQKQ LKEIQWQ LKEIQKQ LK G – NH_2	*c*	QLKEIQ	2835.322
19	4-KE-3.5-N	Ac – G Q LKEIQKQ LKEIQWQ LKEIQKQ LK G – NH_2	*g*	QLKEIQ	3204.785
20	4-KE-3.5-C	Ac – G EIQKQ LKEIQKQ LKEIQWQ LKEIQK G – NH_2	*c*	QLKEIQ	3333.900

Table S1 Identifiers, sequences, registers, heptads and masses (Da) of all discussed peptides. All peptides are in *c*- or *g*-register and are *N*-terminally acetylated and *C*-terminally amidated. Peptides are named for the locations of their charged Glu/Lys residues (1, *e*/*g*; 2, *c*/*e*; 3, *g*/*b*; 4. *b*/*c*), the order of the charged residues in the linear heptad sequence (EK; KE) and the number of heptads in the sequence (3, 3.5 or 4). The exceptions to this naming scheme are CC-Tet,[13] CC-Tet-KE and CC-Tet-3.

Peptide	MRE_{222} at 10 μM ($deg.cm^2.dmol^{-1}.res^{-1}$)	MRE_{222} at 100 μM ($deg.cm^2.dmol^{-1}.res^{-1}$)	Fraction helix at 10 μM (%)	T_M at 10 μM (°C)	Oligomeric state (predicted mass/monomer mass)		Oligomeric state from crystal structure
					SV	SE	
CC-Tet	-35122 ± 616	-35570 ± 193	86	> 95.0	Tri (3.2)	Tet (3.9) *	Tet *
CC-Tet-KE	-34755 ± 389	-35135 ± 296	85	> 95.0	Tri (3.1)	Tri (2.8)	
CC-Tet-3	-16442 ± 405	-27226 ± 588	44	46.6 ± 0.5	Tri (2.9)	Tri (2.7)	
1-EK-4	-32920 ± 1147	-34713 ± 1489	86	> 95.0	Tet (4.0)	Tet (3.7)	
1-KE-4	-35388 ± 1668	-34984 ± 300	93	> 95.0	Tri/Tet (3.5)	Tri/Tet (3.5)	
2-EK-4	-34375 ± 266	-34512 ± 485	90	> 95.0	Tet (3.9)	Tet (3.9)	Tet
2-KE-4	-35277 ± 1472	-34507 ± 643	92	> 95.0	Tet (4.2)	Tet (3.8)	
3-EK-4	-31815 ± 817	-32569 ± 484	83	67.5 ± 0.5	Tet (4.2)	Tet (3.9)	Tet
3-KE-4	-35550 ± 520	-34610 ± 187	92	89.8 ± 1.0	Tet (3.8)	Tet (3.8)	
4-EK-4	-35402 ± 305	-36624 ± 729	93	> 95.0	Tet (4.1)	Tet (4.1)	
4-KE-4	-34804 ± 669	-36253 ±259	91	> 95.0	Tet (4.2)	Tet (4.1)	Tet
1-EK-3	-4690 ± 268	-8062 ± 104	13	< 5.0	N.D. (UF)	N.D. (UF)	
2-EK-3	-12230 ± 420	-27229 ± 525	33	37.2 ± 2.4	Tri/Tet (3.4)	Tri (3.3)	
3-EK-3	-4750 ± 566	-4415 ± 221	13	< 5.0	N.D. (UF)	N.D. (UF)	
4-EK-3	-24853 ± 847	-29900 ± 1525	65	39.7 ± 0.8	Tet (4.0)	Tet (3.7)	
4-EK-3.5-N	-33680 ± 283	-35682 ± 686	88	90.5 ± 1.0	N.D. (P)	N.D. (P)	
4-EK-3.5-C	-31354 ± 490	-33528 ± 549	82	80.3 ± 0.3	Tet (4.2)	Tet (3.9)	
4-KE-3	-25529 ± 859	-31372 ± 322	67	51.7 ± 0.3	Tet (3.8)	Tet (3.8)	
4-KE-3.5-N	-32865 ± 1025	-34409 ± 616	86	84.3 ± 0.8	Tet (4.1)	Tet (3.9)	
4-KE-3.5-C	-34402 ± 354	-37729 ± 780	90	85.7 ±0.3	Tet (3.9)	Tet (4.0)	

Table S2 Biophysical parameters for all discussed peptides. MRE_{222} and fraction helix values were measured at 5°C. T_M values are the midpoints of thermal denaturation determined from the second derivatives of the unfolding curves. Errors are one s.d. from the mean. All CD measurements were performed in PBS (pH 7.4) at 10 or 100 μM peptide concentration. MRE, mean residue ellipticity; SV, sedimentation velocity; SE, sedimentation equilibrium; Mon, monomer; Di, dimer; Tri, trimer; Tet, tetramer; N.D., not determined; UF, not determined because peptide was unfolded; P, precipitated and an oligomeric state could not be determined (This may have been due to the lower pI value of 8.38 for 4-EK-3.5-N. Conversely, the other class-4 peptides all had pI values in the range 9.31–9.88).

Peptide	Buffer	pH	Salt	Precipitant
2-EK-4	0.1 M PCTP	7.0	-	25 % (w/v) PEG 1500
3-EK-4	0.1 M Sodium HEPES	7.5	0.2 M Sodium citrate tribasic dihydrate	20 % (v/v) 2-propanol
4-KE-4	1.6 M Sodium Citrate	6.5	-	-

Table S3 Crystallisation buffer conditions for peptide X-ray crystal structures. PEG, polyethylene glycol; HEPES, 4-(2-hydroxyethyl)-1-piperazineethanesulfonic acid. PCTP: sodium propionate, sodium cacodylate trihydrate, bis-tris propane.

Collection		
Wavelength (Å)		0.9763
Beamline (Diamond, UK)		i03
Space Group		C 2 2 2
Cell Dimensions	a, b, c (Å)	47.56, 50.84, 43.94
	α, β, γ (°)	90, 90, 90
Resolution (Å)		43.94–1.70 (43.94–9.00) [1.73–1.70]
Total reflections		48148 (358) [2382]
Unique reflections		6093 (56) [308]
R_{merge} (within I+/I-)		0.080 (0.109) [0.303]
R_{meas} (within I+/I-)		0.091 (0.129) [0.347]
I/σI		12.8 (52.0) [1.9]
CC ½		0.990 (0.983) [0.978]
Completeness (%)		99.6 (99.4) [100.0]
Multiplicity		7.9 (6.4) [7.7]
Wilson B Factor (Å^2)		19.73
Refinement		
Resolution (Å)		43.94–1.70
Reflections/Unique		12139/6093
R_{work}/R_{free}		0.1826/0.2143
No. atoms	Protein	500
	Water	41
	Ligand/ion	10
B-factors	Main chain/whole chain	20.397/26.568
	Water	44.480
	Ligand	50.611
R.m.s.d	Bond lengths (Å)	0.006
	Bond angles (°)	0.730
Ramachandran (%)	Favoured	100.0
	Allowed	0.0
	Outliers	0.0
Clash score		8.60

Table S4 Data collection and refinement statistics for peptide 2-EK-4 (PDB ID: 6XXZ). Collection statistics shown as overall (inner shell) [outer shell].

Collection		
Wavelength (Å)		0.9795
Beamline (Diamond, UK)		i04
Space Group		P1 21 1
Cell Dimensions	a, b, c (Å)	29.46, 48.55, 36.57
	α, β, γ (°)	90.00, 96.19, 90.00
Resolution (Å)		48.55–1.11 (48.55–6.06) [1.12–1.11]
Total reflections		236063(1645) [9796]
Unique reflections		38599 (265) [1806]
R_{merge} (within I+/I-)		0.051 (0.048) [0.908]
R_{meas} (within I+/I-)		0.062 (0.059) [1.127]
I/σI		12.7 (36.4) [1.9]
CC ½		0.998 (0.995) [0.629]
Completeness (%)		94.5 (99.0) [90.6]
Multiplicity		6.1 (6.2) [5.4]
Wilson B Factor (Å^2)		12.88
Refinement		
Resolution (Å)		29.10–1.11
Reflections/Unique		76792/38574
R_{work}/R_{free}		0.1639/0.1994
No. atoms	Protein	1013
	Water	134
	Ligand/ion	0
B-factors	Main chain/whole chain	15.387/17.785
	Water	40.396
R.m.s.d	Bond lengths (Å)	0.004
	Bond angles (°)	0.620
Ramachandran (%)	Favoured	100.0
	Allowed	0.0
	Outliers	0.0
Clash score		6.69

Table S5 Data collection and refinement statistics for peptide 3-EK-4 (PDB ID: 6XY0). Collection statistics shown as overall (outer shell) [inner shell].

Collection		
Wavelength (Å)		0.9762
Beamline (Diamond, UK)		i03
Space Group		P 43
Cell Dimensions	a, b, c (Å)	53.52, 53.52, 50.28
	α, β, γ (°)	90.00, 90.00, 90.00
Resolution (Å)		53.52–1.50 (53.52–8.22) [1.53–1.50]
Total reflections		256373 (1206) [10241]
Unique reflections		22852 (153) [1106]
R_{merge} (within I+/I-)		0.119 (0.160) [0.138]
R_{meas} (within I+/I-)		0.130 (0.189) [0.156]
I/σI		25.1 (26.8) [13.4]
CC ½		0.995 (0.918) [0.992]
Completeness (%)		100.0 (97.0) [100.0]
Multiplicity		11.2 (7.9) [9.3]
Wilson B Factor (Å^2)		11.48
Refinement		
Resolution (Å)		37.84–1.50
Reflections/Unique		45636/22824
R_{work}/R_{free}		0.1612/0.1883
No. atoms	Protein	1059
	Water	160
	Ligand/ion	0
B-factors	Main chain/whole chain	13.145/15.532
	Water	29.081
R.m.s.d	Bond lengths (Å)	0.006
	Bond angles (°)	0.740
Ramachandran (%)	Favoured	100.0
	Allowed	0.0
	Outliers	0.0
Clash score		6.73

Table S6 Data collection and refinement statistics for peptide 4-KE-4 (PDB ID: 6XY1). Collection statistics shown as overall (outer shell) [inner shell].

SUPPLEMENTARY REFERENCES

(1) Myers, J. K., Pace, C. N., and Scholtz, J. M. (1997) A direct comparison of helix propensity in proteins and peptides. *Proc. Natl. Acad. Sci. U.S.A. 94*, 2833-2837.

(2) Brown, P. H., and Schuck, P. (2006) Macromolecular size-and-shape distributions by sedimentation velocity analytical ultracentrifugation. *Biophys. J. 90*, 4651-4661.

(3) Battye, T. G. G., Kontogiannis, L., Johnson, O., Powell, H. R., and Leslie, A. G. W. (2011) iMOSFLM: a new graphical interface for diffraction-image processing with MOSFLM. *Acta Crystallogr. D 67*, 271-281.

(4) Evans, P. R., and Murshudov, G. N. (2013) How good are my data and what is the resolution? *Acta Crystallogr. D 69*, 1204-1214.

(5) Mccoy, A. J., Grosse-Kunstleve, R. W., Adams, P. D., Winn, M. D., Storoni, L. C., and Read, R. J. (2007) Phaser crystallographic software. *J. Appl. Crystallogr. 40*, 658-674.

(6) Kantardjieff, K. A., and Rupp, B. (2003) Matthews coefficient probabilities: Improved estimates for unit cell contents of proteins, DNA, and protein-nucleic acid complex crystals. *Protein Sci. 12*, 1865-1871.

(7) Wood, C. W., Heal, J. W., Thomson, A. R., Bartlett, G. J., Ibarra, A. A., Brady, R. L., Sessions, R. B., and Woolfson, D. N. (2017) ISAMBARD: an open-source computational environment for biomolecular analysis, modelling and design. *Bioinformatics 33*, 3043-3050.

(8) Wood, C. W., and Woolfson, D. N. (2018) CCBuilder 2.0: Powerful and accessible coiled-coil modeling. *Protein Sci. 27*, 103-111.

(9) Rodriguez, D. D., Grosse, C., Himmel, S., Gonzalez, C., de Ilarduya, I. M., Becker, S., Sheldrick, G. M., and Uson, I. (2009) Crystallographic ab initio protein structure solution below atomic resolution. *Nat. Methods 6*, 651-653.

(10) Winn, M. D., Ballard, C. C., Cowtan, K. D., Dodson, E. J., Emsley, P., Evans, P. R., Keegan, R. M., Krissinel, E. B., Leslie, A. G. W., McCoy, A., et al. (2011) Overview of the CCP4 suite and current developments. *Acta Crystallogr. D 67*, 235-242.

(11) Emsley, P., Lohkamp, B., Scott, W. G., and Cowtan, K. (2010) Features and development of Coot. *Acta Crystallogr. D 66*, 486-501.

(12) Adams, P. D., Afonine, P. V., Bunkoczi, G., Chen, V. B., Davis, I. W., Echols, N., Headd, J. J., Hung, L. W., Kapral, G. J., Grosse-Kunstleve, R. W., et al. (2010) PHENIX: a comprehensive Python-based system for macromolecular structure solution. *Acta Crystallogr. D 66*, 213-221.

(13) Fletcher, J. M., Boyle, A. L., Bruning, M., Bartlett, G. J., Vincent, T. L., Zaccai, N. R., Armstrong, C. T., Bromley, E. H. C., Booth, P. J., Brady, R. L., et al. (2012) A Basis Set of de Novo Coiled-Coil Peptide Oligomers for Rational Protein Design and Synthetic Biology. *ACS Synth. Biol. 1*, 240-250.